Krittika Summer Projects 2024

# Binary Black Holes from Scratch

Gokularamanan R S, 23B1854

KRITTIKA SUMMER PROJECTS 2024

# Binary Black Holes from Scratch

Gokularamanan R S, 23B1854[1]

[1]IIT Bombay


PUBLISHED BY KRITTIKA: THE ASTRONOMY CLUB OF IIT BOMBAY
GITHUB.COM/KRITTIKAIITB
Sample Repository: Binary Black Holes from Scratch
Instructions document
First Release, August 2024

# Foreword

This end-term report contains my understanding of stellar evolution - single star evolution and binary star evolution, and a basic introduction to COMPAS, covering some of the really nice and useful utilities that it offers. Along with this, I have also provided my explanations, observations and conclusions derived from the post-processing of the COMPAS outputs generated for Tasks - 0,1,2,3,4 and 5, as given in the instructions document.

Further, I have also added all my code for processing the COMPAS Outputs, generating plots and even a copy of all the plots on my GitHub repository : `https://github.com/ramanan849/BBHs_from_scratch_KSP5.0`

# Contents

# 1. Single Star Evolution

## 1.1 Introduction

The process of change that a star undergoes, from its birth from a cloud of gas and dust to its death, when it is no longer considered a star (in the usual sense), is called "**stellar evolution.**"
Stars take millions of years to evolve. We humans cannot physically track down the evolutionary stages of stars. Hence, we use alternative methods to study them in detail. One way we can track them down, is by studying variable stars.
*Variable stars*, unlike other stars, do change on timescales that we can observe. These stars have a variation in their brightness. This provides us with many properties that we can study about them - luminosity, period, etc., all these can provide us answers about the star's evolution. Studying them gives us crucial information about how stars change over millions of years.

## 1.2 From birth till demise : Various stages of a star's life

1. Protostar (Pre Main Sequence)
2. Main Sequence (MS)
3. Post Main Sequence
4. Old age
5. Death

## 1.3 How are stars studied?

First of all, before going to learning about the various evolutionary states of star, it is highly important to know how different physical properties of stars - such as mass, age, core temperature, density, etc are known.

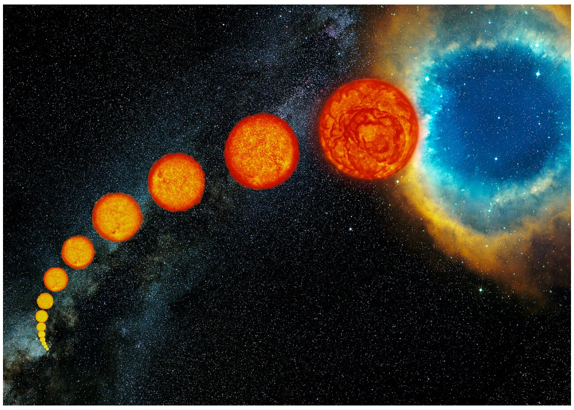

Figure 1.1: Credit: AAVSO

### 1.3.1 Astroseismology

1. We study the interior of stars, find their mass, age, density of core, the temperature inside and other properties by analyzing the vibrations that we record from them. These *"vibrations"* are measured by observing the *variations in brightness of different parts of the star's surface.*
2. These vibrations are called "**pulsations**". In all stars, there are a lot of different vibrations happening at the same time. Each *vibration frequency* is called a "**pulsation mode**". If we can combine information about each of these different modes into a single model that can explain them all, then this model can tell us a great deal about the inside of the star.
3. Helioseismology : Study of the Sun's pulsations. However, there're other variations that occur on the Sun's surface:
   (a) Sun spots - caused by strong magnetic fields on the Sun that interfere with heat transfer from the Sun's interior to the surface. This results in cooling down of the part of the surface which doesn't receive the heat. This in turn, makes the spot darker.
   (b) Solar flares - also associated with magnetic fields around sunspots, and are caused by these magnetic fields acting like giant particle accelerators, squeezing the gas in the solar atmosphere and accelerating it to great speeds.

### 1.3.2 Hertzsprung-Russell Diagram (HR Diagram)

1. It is one of the most important tools used in the study of stellar evolution. Developed by the early $20^{th}$ century century astronomers Ejnar Hertzsprung and Henry Norris Russell, it plots the **temperature of stars against their luminosity** (the theoretical HR diagram), or **the colour of stars (or spectral type) against their absolute magnitude** (the observational HR diagram, also known as a colour-magnitude diagram).
2. Depending on its initial mass, every star goes through specific evolutionary stages dictated by its internal structure and how it produces energy. Each of these stages corresponds to a change in the temperature and luminosity of the star, which can be seen to move to different regions on the HR diagram as it evolves. This reveals the true power of the HR diagram – astronomers can know a star's internal structure and evolutionary stage simply by determining

its position in the diagram.

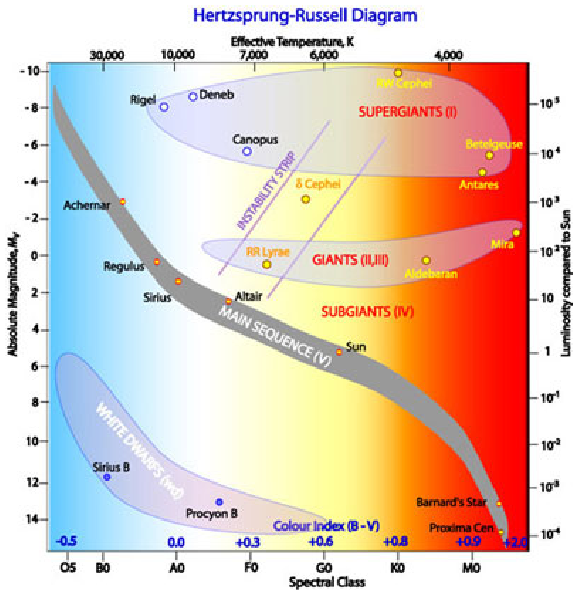


Figure 1.2: Credit: R. Hollow, CSIRO.

3. There are 3 main regions (or evolutionary stages) of the HR diagram:
   (a) The main sequence (gray region) (ref. 1.5) stretching from the upper left (hot, luminous stars) to the bottom right (cool, faint stars) dominates the HR diagram.
   (b) Red giant and supergiant stars (ref. 1.6) (luminosity classes I through III) occupy the region above the main sequence.
   (c) White dwarf stars (ref. 1.8.1) (luminosity class D) a are found in the bottom left of the HR diagram. These stars are very hot but have low luminosities due to their small size.

## 1.4 Pre-Main Sequence

1. Star birth begins with the gravitational collapse of giant molecular clouds (really massive, can weigh upto millions of $M_\odot$). As it collapses, the molecular cloud, also called "nebulae" break down into smaller fragments and in each of these fragments, the collapsing gas releases gravitational potential energy as heat. As the temperature and pressure increase, a fragment condenses into a rotating sphere of superhot gas known as **protostar**.
2. The nascent star (protostar) is still forming, the accretion of mass onto the star from the gas cloud is still not over.
3. Some of the most remarkable of these young stars are the Orion/Nebular variable stars. One such class of variables are *T Tauri* stars, which are extreme in their variability. They exhibit such variability due to their active accretion process. Other Orion variables include FUORs (FU Orion stars) and UXORs (UX Orion stars). FUORs are known to accrete matter at very rapid rates.

## 1.5 Main Sequence

1. Once the star has completed accretion of all the gas and dust from the clouds that it formed from, it enters *Main Sequence*, the major part of its life.
2. During this period, the star stars fusing hydrogen into helium in its core and produces heat, light and energy.
3. More than $90\%$ of the stars in the universe are in Main Sequence. (ref. 1)
4. The MS lifetime is mainly a function of the star's mass. Heavier stars stay shorter in the Main Sequence than lighter stars.

$$\text{MS lifetime of star} \propto \frac{1}{\text{Mass of star}}$$

5. Protostars with masses less than roughly $0.08MSun$ ( $1.6 * 10^{29}$ kg) never reach temperatures high enough for fusion of hydrogen to begin. These are known as **brown dwarfs**. In such stars, there may be fusion of Deuterium in them at some point; however, they slowly die away by cooling over hundreds of millions of years.
6. **Note**: The initial mass of the star is the mass that the star has at the start of its Main Sequence (Zero age Main sequence, or ZAMS). As the star ages, it tends to lose a lot of its mass.

## 1.6 Post Main Sequence

1. Once stars have exhausted their hydrogen fuel in their cores, nuclear fusion of Hydrogen ceases and burning of Helium and other elements begins. The core collapses onto itself, the outer surface, due to lack of heat, starts expanding and becomes darker and redder (Surface area increases and surface temperature becomes less than 4100 K). The star becomes a red giant => It enters RGB era (Red-Giant Branch).
2. RGB stars still give off light due to presence of remnant energy from nuclear fusion.
3. The Post-MS lifetime of a star is much less compared to its MS lifetime (on a stellar scale).
4. Post MS stars **lying in the instability strip of the HR diagram may pulsate** (be variable). Most important of all such pulsating post MS stars are the ***Cepheid variable stars***. Other such pulsating variables include : *delta Scuti* and *RR Lyrae*.
   (a) Cepheid variables are massive stars and they vary in brightness based on their pulsating periods, which are linked to their luminosity.
   (b) Cepheids, delta Scuti and RR Lyrae follow the **Leavitt's law** :

$$\text{luminosity (or) absolute magnitude} \propto \text{period}$$

$$m = \alpha + \beta * (\log(P) - 1)$$

(period, P = time taken to complete one pulsation period and m = absolute magnitude, alpha and beta are parameters)

## 1.7 Far from Post Main Sequence

Last stage of stellar evolution where a star is truly a "star" (looks like a star - spherically shaped, emits light, reddish in colour)

*Star (MS) →RGB →Red Clump (Population I stars) / Horizontal branch (Population II stars)→Stars that are fusing Helium to Carbon in their cores*

1. Stars eventually run out of all their fuel and come out of the RGB phase. Then, they either become a part of Population I / II stars, depending upon their temperatures.
2. This phase that the star enters is called AGB - Asymptotic Giant Branch. In AGB phase, shells of hydrogen (remaining) and helium start burning and are closer to the surface. Due to this reason, the star appears very luminous and increases in size. However, the temperature is much lower than compared to MS. Hence, AGB stars appear more redder.
3. AGB stars also undergo occasional events, called "**thermal pulses**" where the layer of helium surrounding the core suddenly undergoes thermonuclear burning. This causes large changes to the star's luminosity and temperature.
4. (Time spent in AGB) $<<<$ (Time spent in RGB).
5. One of the most famous AGB stars is the class of stars : ***Mira variables.*** They are giant pulsating stars that take 100 or more days to complete one pulsation. Everything about Mira variables is large - large periods, large magnitudes ($\geq 2.5$)

## 1.8 Compact objects

Once nuclear fusion of material in a star stops altogether, the star lose the balance (hydrostatic equilibrium - outward radiation balances the gravity pulling in - **no more of this equlilibrium**) and its core collapses. This leaves behind a dead star (compact object).
Finally, whatever is left behind depends on the mass at ZAMS (M-ZAMS):

1. If M-ZAMS $< 8*$M-Sun, then a white dwarf
2. $8*$M-Sun $<$ M-ZAMS $< 20*$M-Sun, then a neutron star
3. If M-ZAMS $> 20*$M-Sun, then a black hole

### 1.8.1 White Dwarf

1. Powerful winds due to clouds of gas pushes the star and as a result, matter begins to blow away and outer layers get ejected from the star. At this stage, the star appears more diffuse and nebular in nature (planetary nebula) and exposes a small, dense, white core, called "**white dwarf**".
2. White dwarfs are very hot when formed but there is no source of energy and hence, it will slowly cool down.
3. They are prevented from collapsing (due to gravity) by degenerate electron gas, which is stiff as solid.

Figure 1.3: A white dwarf, Credit: Space.com

### 1.8.2 Neutron Star

1. Once the mass of a white dwarf exceeds ($1.4 *$ M-Sun) (Chandrasekhar's limit), the core of a massive star collapses by overcoming electron degeneracy forces. Huge amount of energy is released - big *supernova explosion*.
2. The supernova compresses the core even further until its collapse is halted by neutron degeneracy pressure. If the total mass of this core is less than 3 $M_{\odot}$, this results in a *Neutron Star.*
3. Neutron stars are known to have very high rotation speeds and very, very high densities, which also gives them very high surface gravity. In fact, they have escape velocities of over half the velocity of light.
4. *Pulsars* and *Magnetars* are variable neutron stars. Pulsars rotate 100s of times per second on their axes and their magnetic poles emit strong EM radiation as result of rotating in and out of view. This causes their variability. Magnetars have powerful magnetic fields that undergo enormous outbursts at high energies, which travel throughout the Milky way.

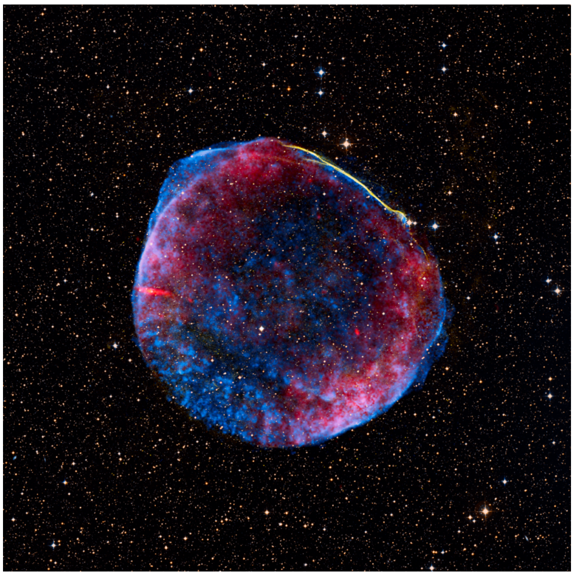

Figure 1.4: Supernova SN1006, Credit: WSU Dept. of Physics and Astronomy

### 1.8.3 Black Hole

1. During the supernova explosion, if the compressed core of the star exceeds $3\,M_\odot$, then its collapse cannot be halted (gravity outweighs everything). This results in the creation of a *black hole*.
2. Black holes have such strong gravitational fields that their escape velocities are larger than the speed of light.
3. After a black hole has formed, it can grow by absorbing mass from its surroundings.

# 2. Binary Star Evolution

## 2.1 Binary stars

A binary star system is one in which 2 stars are gravitationally bound to each other and orbit around a common centre of mass. They are of immense importance to astronomers as they allow the masses of stars to be determined. In reality, almost 85 percent of all stars in the universe are found in binary systems. Our Sun is among the 15 percent which doesn't have a companion.

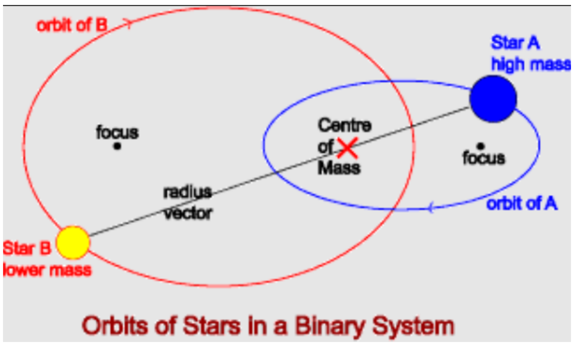


Figure 2.1: A binary star system, Credit: ATNF CSIRO

## 2.2 Types of binaries

1. Visual binaries -
   (a) They are the most prominent ones in the sky. The component stars can be resolved and seen through telescopes and are physically separated by 10-100 AU (1 AU = $\approx 1.4959 * 10^{11} m$)
   (b) $\alpha$ Centauri A and $\alpha$ Centauri B are visual binaries
2. Spectroscopic binaries -

(a) They cannot be properly resolved by a telescope. They are too distant to be called "visual" binaries.
(b) They are detected by Doppler shifts in their spectral lines.
(c) This spectrum of a binary system contains 2 components - 1 from each star. Suppose a binary contains stars A and B. If A is moving away and B is moving towards us, then the spectrum of A will be on the red-end (longer wavelength) and that of B will be on the blue-end (shorter wavelength). As they orbit, their directions change with respect to us, hence their spectrum shift to the opposite sides (A on the blue-end and B on the red-end now).

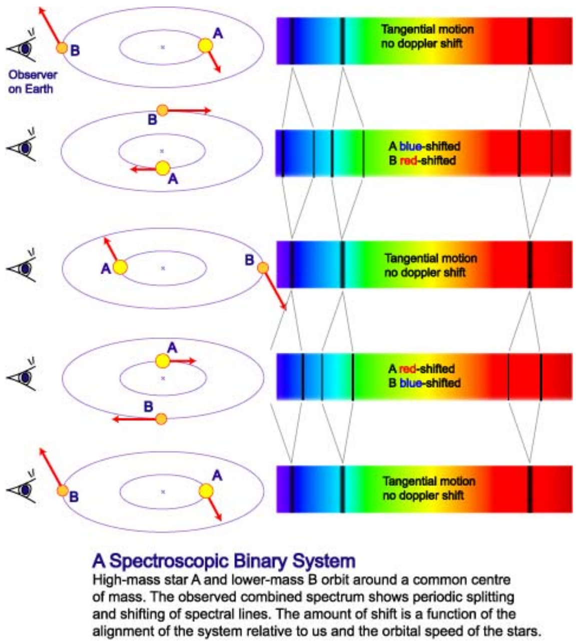


Figure 2.2: Credit: ATNF CSIRO

3. Eclisping binaries -
   (a) Binary stars eclipse each other every time they cross each in orbit. This causes a change in the eclipsed star's brightness. We record the **light curves** (plot of Apparent Magnitude vs Time) during these "eclipses".
   (b) Analysis of **light curves** provides us with:
      i. eccentricity
      ii. orientation
      iii. inclination of the orbit
      iv. radii of the stars relative to the orbit size
      v. ratio of the effective temperature of stars, etc.
   (c) One of the notable eclipsing binaries involve the Algol variables, which is the first ever recorded eclipsing binary. Studies of the eclipsing Algol variables led to the **Algol Paradox** (refer subsection 5)
4. Astrometric binaries -
   (a) If we repeatedly observe some stars over a long time, they show a *"perturbation or wobble"* in their proper motion. If these perturbations are periodic, then these occur due to the gravitational influence of an unseen companion, which leads to the fact that the stars are in a binary

system.

(b) 2.3 Sirius A and Sirius B form a astrometric binary.

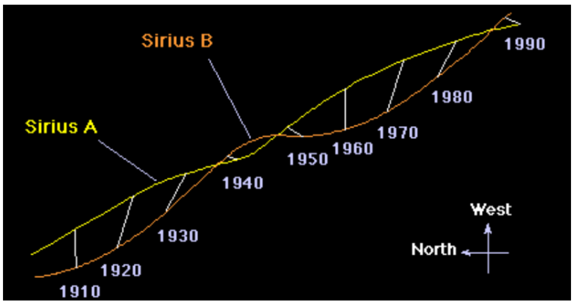


Figure 2.3: Astrometric binary : Sirius A is brighter and larger while Sirius B is smaller and colder. Perturbations observed at regions of intersections
Credit: ATNF CSIRO

## 2.3 Evolution of binary star systems

Most binaries develop during star formation. The fragmentation of the molecular cloud (refer, nebulae 1.4) during the formation of protostars is an acceptable explanation for the formation of a binary or multiple star system. The individual stars evolve as per Single Star Evolution until they undergo **mass transfer**.
There is also the three-body

### 2.3.1 Mass transfer

1. This is one of the most important events in a binary star system. Mass transfer can change the way stars evolve as the evolution of stars is determined by their masses.
2. The gravitational fields between the two stars get complicated. As each of the stars enters main sequence, they keep increasing in size.
3. Visualizing the gravitational fields around the stars as topographic map (refer Fig 2.5), there's a contour line separating the two stars which balances the gravitational pull of each star (*null point*). It serves as a equipotential surface and is called as "**Roche lobe**". Any mass that rests on this equipotential surface is equally pulled by each star. Now, if a star grows such that it exceeds its *Roche lobe*, then some of its matter ventures into a region where the gravitational pull of its companion star is larger than its own. As a result, matter will transfer from the first star to its companion through a process known as **Roche lobe overflow (RLOF)** (commonly called mass transfer), either being absorbed by direct impact or through an accretion disc.
4. It is also possible that if a star grows out of its Roche lobe too fast for all abundant matter to be pulled by its companion, matter will leave the system as *stellar winds*, thus being effectively lost to both stars.
5. **Algol Paradox**: It is known that massive stars evolve much faster than the less massive ones. However, it was observed that the more massive component Algol A was still in the main sequence, while the less massive Algol B became a subgiant (The subgiant branch is a stage in the evolution of low to intermediate mass stars, post main sequence) at a later evolutionary stage.

This paradox can be solved by *mass transfer*: When the more massive star (Algol A) becomes massive enough to overflow its Roche lobe, most of its mass gets transferred to its companion, the less massive star (Algol B), which is still in the main sequence. As a result, Algol A gets an extended Main Sequence lifetime, while Algol B's time on MS shortens and it soon leaves MS to become a subgiant.
As seen in the Algol variables case, mass transfer indeed alters the evolution trajectory of binary stars

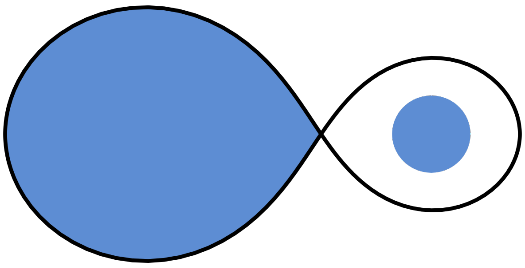

Figure 2.4: Mass transfer in a semi-detached binary system where the star on the left has filled its Roche lobe while the one on the right has not. This results in transfer of mass from the star on the left to the one on the right, Credit: Wikipedia

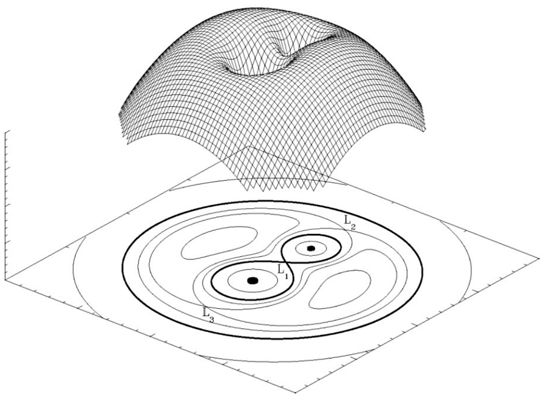

Figure 2.5: A three-dimensional representation of the Roche potential in a binary star system with mass ratio 2, Credit: Wikipedia

#### Unbound binary

Now, it is also possible for widely separated binaries to lose gravitational contact with each other during their lifetime as a result of external perturbations. The components will then move on to evolve as single stars. This leads to an **unbound binary**.

**White dwarf explosions**

If a white dwarf has a close companion star that overflows its Roche lobe, the white dwarf will steadily accrete gases from the star's outer atmosphere. These are compacted on the white dwarf's surface by its intense gravity, compressed and heated to very high temperatures as additional material is drawn in. This results in something called a "**nova**".

### 2.3.2 Stable mass transfer

1. Here, most, but not necessarily all, of the transferred mass is accreted by the companion star, generally leading to a widening of the binary.
2. Mass transfer ends when most of the hydrogen-rich envelope of the donor star has either been transferred to the companion or been lost from the system.
3. Mass accretion will also change the structure of the accreting star. If it is still on the main sequence, the accretor tends to be rejuvenated and then behave like a more massive normal main-sequence star. On the other hand, if it has already left the main sequence, its evolution can be drastically altered, and the star may never evolve to become a red supergiant, but explode as a blue supergiant (if it is a massive star).

**Conservative mass transfer**

This is where all the mass lost by the donor is accreted by the companion, and the total angular momentum of the binary is conserved.

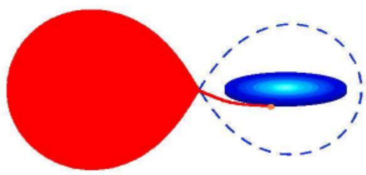

Figure 2.6: Stable mass transfer, Credit: Ph Podsiadlowski

### 2.3.3 Unstable mass transfer

Mass transfer is unstable when the accreting star cannot accrete all off the material transferred from the donor star. The transferred material then piles up on the accretor and starts to expand, ultimately filling and overfilling the accretor's Roche lobe. This leads to the formation of a **common-envelope** (CE) system, where the core of the donor and the companion form a binary immersed in the envelope of the donor star. (Refer Fig. 2.7)

### 2.3.4 Old age and death of binary stars

Due to mass transfer, there are multiple possibilities of how a binary can end - what type of compact objects are formed, whether the binary would still be bound, would there be mergers of objects, etc. The following are the possible states an ***intact*** binary could be in wherein either of the stars have become a compact object (WD - White Dwarf, NS - Neutron Star, BH - Black Hole) :

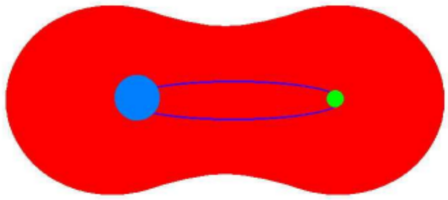

Figure 2.7: Unstable mass transfer, Credit: Ph Podsiadlowski

1. WD + WD - A binary wherein both the stars are not massive enough to evolve further than WD (each of their masses as a white dwarf is less than 1.4 times the solar mass). A peaceful outcome.
2. WD + NS - A binary where there has been mass transfer and heavier star has underwent a supernova explosion to become a neutron star while its less massive companion has become a white dwarf.
3. NS + NS - A binary where both massive stars have underwent supernova explosions to become two supernovae.
4. NS + BH - A binary where a supermassive star (mass greater than 20*solar mass) undergoes a supernova explosion to become a black hole, while its less-massive companion (still a massive star) undergoes another supernova explosion but to become a neutron star.
5. BH + BH - A binary where there are two supermassive stars, both of which end up as black holes.

### 2.3.5 Binary mergers

Very rare and special stellar events wherein 2 compact objects in a binary system, which are surprisingly very close, collide and merge. Such mergers of compact objects are detected by LIGO and VIRGO detectors on Earth, which observe gravitational waves and short GRBs.

1. White dwarf merger -
   (a) In a WD+WD binary, both the white dwarfs come closer, with the less massive white dwarf spirals close in to its more massive counterpart.
   (b) Gravitational tidal forces disrupt the less massive star because it is physically larger and more easily stretched by the intense gravity of the compact companion white dwarf.
   (c) Though most of the material falls directly onto the white dwarf, some spreads into a broad flattened disk. New planets can form on this disk.
2. Neutron star merger -
   (a) Happens in NS+NS binaries. Each neutron star gradually spiral inward due to gravitational radiation (generated by the accelerated masses of objects in a binary system). When they finally meet, their merger leads to the formation of either a **more massive neutron star**, or—if the mass of the remnant exceeds the **Tolman–Oppenheimer–Volkoff limit** (specifies the upper limit of the mass of a neutron star, which is in the range of 2.2 to 2.9 $M_{\odot}$, 'current agreed range') —a **black hole**.

   **Note!! : COMPAS considers all NS to have masses < 2.5 MSun** (source: `https://compas.readthedocs.io/en/latest/pages/User%20guide/Post-processing/`

CHE_paper_tutorial/CHE_evolution_demo_ANSWERS.html#Question-2:)

(b) The merger can create a magnetic field that is trillions of times stronger than that of Earth in a matter of one or two milliseconds.

(c) These events are believed to create **short gamma-ray bursts** (short GRBs)(have duration of less that 2 seconds; the most energetic form of light). They are also known to produce "kilonovae", bright blasts of EM radiation due to radioactive decay of heavy elements that are created from the merger.

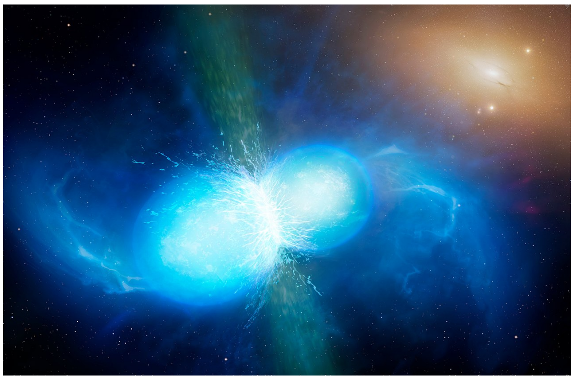

Figure 2.8: Artist's impression of neutron stars merging and producing gravitational waves, Credit: Wikipedia

3. Neutron star - Black Hole merger -
   (a) Very rare even among other mergers. Happens in NS+BH binaries.
   (b) Likely that the merger results in a bigger black hole and emission of powerful gravitational waves.
4. Black hole merger -
   (a) Happens in BH+BH binaries.
   (b) The merger results in the formation of a bigger black hole along with emission of powerful gravitational waves.

## 2.4 GW observations of merging binaries:

Gravitational-wave (GW) observations of merging binaries, such as those detected by LIGO and Virgo, provide a wealth of information about the stellar and binary evolution that preceded the mergers. The gravitational-wave signature encodes the properties of the merging binary black holes: the component masses and spins. Some of the questions that it can answer:

1. Stability and Consequences of Mass Transfer
2. What can gravitational-wave observations of merging binaries tell us about the stellar and binary evolution that preceded the mergers?
3. Can the observations constrain the amount of mass loss and expansion experienced by massive stars?
4. Does the redshift distribution of merging compact objects contain an imprint of the star formation history of the Universe

# 3. COMPAS

Compact Object Mergers: Population Astrophysics and Statistics

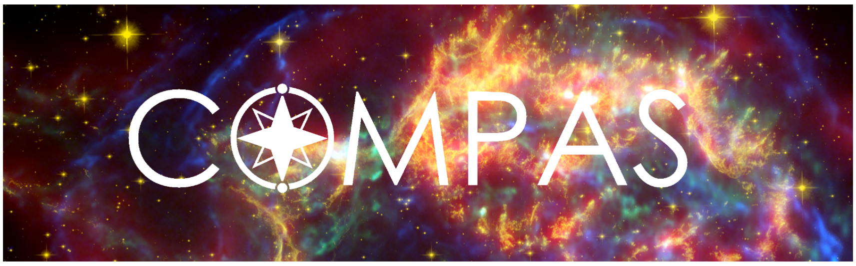


Figure 3.1: Source: `https://compas.science/index.html`

- COMPAS is a rapid stellar / binary population synthesis code that can simulate stars / binary stars according to the user's choice of model parameters.
- It draws properties for a binary star system from a set of initial distributions, and evolves it from zero-age main sequence to the end of its life as two compact remnants. It has been used for inference from observations of gravitational-wave mergers, Galactic neutron stars, X-ray binaries, and luminous red novae. (source : `https://compas.science/index.html`)

- COMPAS could be run in 3 ways, via:
  - Command line :
    * Directly runs COMPAS along with the parameters that need to be adjusted.
    * Suitable for simulations where the parameters are adjusted such that no set of binaries/stars require some specific parameters and other set of binaries/stars require some different set of parameters.
    * For example,

./COMPAS -n 200 –random-seed 4512 –initial-mass-max 200 –detailed-output -c exfolder_name -o ./example_path/

Here,

# **./COMPAS** is used to execute the COMPAS.sh script and finally returns a HDF5 file named by default as "COMPAS_Output.h5".
# The parameter **-n** denotes the number of binaries that we want to simulate.
# **–random-seed**
# **–initial-mass-max** gives the maximum initial mass (at ZAMS) limit of stars in terms of $M_{\odot}$.
# **–detailed-output** provides a detailed output of the simulation, which includes files such as "BSE_Detailed_Output.h5" which can be processed later to generate HR diagrams, diagrams that illustrate the evolutionary stages of a binary star system, right from ZAMS and covers MT events, mergers, SN events, DCO formation, etc. (ref: Task1 (4.1))
# **-c** tells COMPAS to name the folder containing the .h5 files with the provided name (here, "exfolder_name")
# **-o** redirects COMPAS to save the folder created in the above step to a particular directory (the default is /COMPAS/SRC/). Here, it tells COMPAS to save it in the directory /COMPAS/SRC/example_path/ .

– Python
  * Suitable for runs with wide variations in adjustments of parameters. For example, (take a very basic example) say we're simulating 20 binaries, each with different masses. In such a case, running COMPAS via Python would be more suitable compared to the command line
  * A Python file named "runSubmit.py" is used, along with a txt file called grid-file that contains the different parameters for each set of binaries that we would like to generate. Further, instead of using a grid-file, we can also use a config file - a .yaml file which contains all the parameter configuration that COMPAS offers at one place.

– Docker (this is a method that I haven't tried)

- Some helpful utilities offered by COMPAS that I used in the project:

1. **printCompasDetails()** : A python function that prints the entire data related to each of the keys of the COMPAS_Output.h5 file in a nice looking Pandas dataframe.

2. **getEventHistory()** and **getEventStrings()**: As the names suggest, these functions provide data related to all the MT and SN events that happen in a binary star system.
   (a) The getEventHistory() provides data in the form of a nested List.
      i. For example, for the binary 1718628387, the following is the output: **((’MT’, 7.332831999705, 2, 1, True, False, False), (’SN’, 8.239101314130997, 8, 14, 1, False), (’MT’, 11.604925884559995, 14,**

**2, False, True, False), ('SN', 12.416885809407988, 8, 14, 2, False))**.

ii. For 'MT' events, the template is ('MT', time, stellarType1, stellarType2, isRlof1, isRlof2, isCEE).

iii. For 'SN' events, the template is (`SN', time, stellarTypeProgenitor, stellarTypeRemnant, whichIsProgenitor, isUnbound).

iv. For some binaries which do not have any MT and SN events, any tuple () gets displayed.

(b) Coming to getEventStrings(), this provides a string for each binary.

i. For example, for the same binary 1718628387, the EventString is **'2>1_8*I14_14<2_14*I8'**.

ii. For 'MT' events, the options are **P>S, P<S, or P=S** (where P is primary type, S is secondary type, and >, < is RLOF (1->2 or 1<-2) or = for CEE)

iii. For 'SN' events, the options are **P*SR** for star1 the SN progenitor, or **R*SP** for star2 the SN progenitor (where P is progenitor type, R is remnant type, S is state (I for intact, U for unbound).

iv. Now, coming back to the event string for binary 1718628387, '2>1' signifies that star1 of stellar type '2' initiates RLOF towards star2 of stellar type '1'.
Then, '8*I14' says that star1 (now at stellarType 8) is the progenitor (initiates SN) and its remnant is of stellarType 14 and after this SN event, the binary is still intact ('I'). Next, '14<2' tells there is another MT event, now from star2 (stellarType = 2) to star1 (now a NS, stellatType - 14). At last, '14*I8' - we have another SN event, here, star2 (now at stellarType = 8) initiates the SN.

3. **h5copy.py** - It is a python program to combine multiple HDf5 files into one. Used it for very very big simulations (like 100,000 or 1,000,000 binaries in parallel, i.e., for example, ran 10 sets of 10,000 binaries to get 100,000 in total in a time equal to the simulation of 10,000 binaries - ref **Task-4** (4.5) and **Task-5** (4.6)). The syntax is (for command line usage):
*python3 h5copy.py set-1/set1.h5 set-2/set2.h5 ..... set-10/set.h5 -o ./consolidated-file.h5* .

# 4. Explanations to Tasks

https://github.com/ramanan849/BBHs_from_scratch_KSP5.0 - Repository containing Jupyter notebooks and plots for Tasks 0,1,2,3,4 and 5.

## 4.1 Task 1

Run a single binary with detailed evolution turned on. Plot the evolution with the detailed evolution plotter. Be prepared to show the plot you created, and describe the major events in its life.

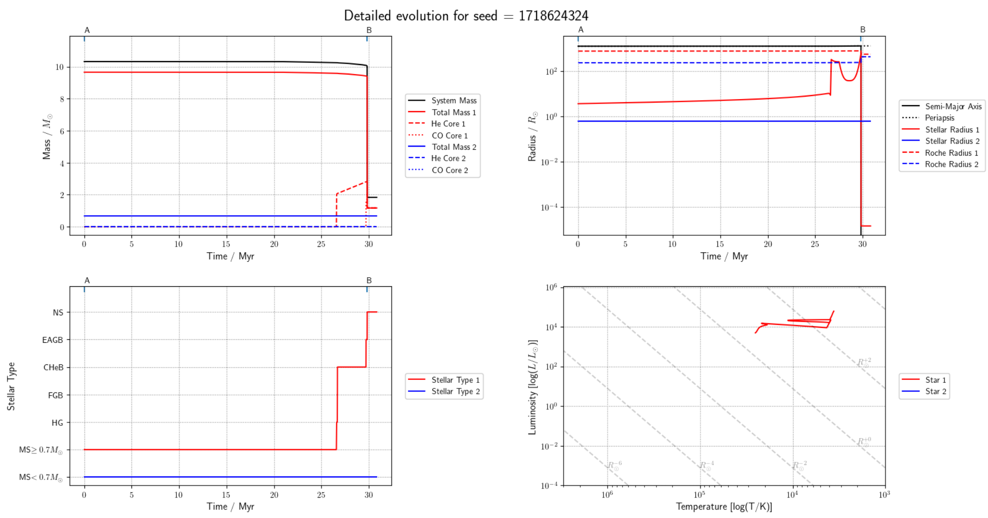


Figure 4.1: Detailed Output Plots for Evolution of a single binary
( I have got one of a kind binary O_O )

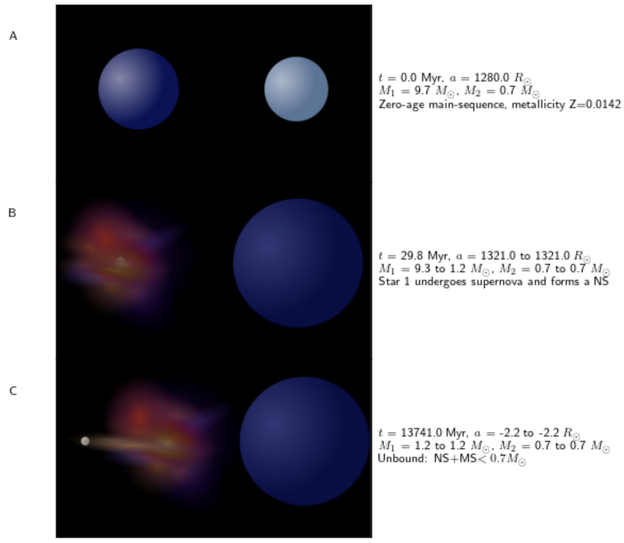


Figure 4.2: Snapshots of some evolutionary steps of the binary

From the first plot - Mass vs Time (top left) and comparing that with Fig.4.2,

1. Star 1, having mass at ZAMS equal to 9.7 $M_\odot$ can be classified as a *massive star* and star 2, having mass at ZAMS equal to 0.7 $M_\odot$ is a **red dwarf** (smallest kind of star on the main sequence). Judging from this plot, there seem to be no events of mass transfer. **So, it can be concluded that the binary 1718624324 is detached** (i.e, each component star is within its Roche lobe, so no possibility of mass transfer).
2. From the fact that lighter stars spend more time on main sequence compared to heavier stars, the **mass and size** of star 2 doesn't change throughout the run-time of the COMPAS simulation, which is 13471 Myr. This is why there's a flat line for star 2 in plot 1, plot 2 (Radius vs Time) and plot 3 (Stellar Type vs Time).
   (a) In plot 1, 2 and 3, it can be seen that star 1 evolves just like a single star. Especially, in plot 2, right from 0 to a little over 25 Myr, star-1's radius increases and it also has the *characteristic main sequence hook* . After that, its radius rapidly increases. At one point, it goes from about 50 solar radii to more than 100 solar radii in a few million years.
   (b) Likewise, in plot 3, star 1 reaches CHeB (Core Helim Burning) from MS in less than a million years. From CHeB, it reaches AGB in under 5 million years. This signifies how short the post-MS period is for massive stars.
   (c) After that, by 28-29 Myrs since start, star 1 starts shedding mass to become a white dwarf. Soon after, it undergoes supernova explosion (its ZAMS mass = 9.7 $M_\odot \in [8, 20]\ M_\odot$) to form a neutron star.
   (d) The binary now containing a newly formed neutron star and a red dwarf still on main sequence, probably experiences some external perturbations and as a result, the gravitational interactions between each component becomes weaker to the extent that the binary becomes

*unbound*. The red dwarf continues its evolution while the neutron star keeps spinning and spinning.

3. Coming to the HR diagram (plot 4), no point/streak of line can be seen for star 2. This is possible because of it being a red dwarf - less luminous, hardly undergoes any evolutionary changes in the first 29.8 million years, has an enormous lifetime on main sequence.

## 4.2 Task 2

Run 10,000 binaries and record how long it took. From the output, determine the fraction of these binaries that (1) Never interact (2) experience unstable mass transfer (or Common Envelope Evolution) (3) experience only stable mass transfer (4) undergo a stellar merger. These will be your dominant channels, though there may be some others - can you identify these? What fraction of your systems experience 0, 1, or 2 supernova explosions, and what kinds of explosions do you see?

The results:

1. The time it took to record the simulation of 10,000 binaries is 225.996 CPU seconds
2. Fraction of binaries that never interact = 0.4112
3. Fraction of binaries that experience unstable mass transfer (or CEE) = 0.4548
4. Fraction of binaries that experience **only** stable mass transfer = 0.1340
5. Fraction of binaries that undergo stellar merger = 0.3086
6. Total number of supernovae = 5432 out of 10,000 (fraction = 0.5432)
   (a) Fraction of binaries with 0 supernovae = 0.6216
   (b) Fraction of binaries with 1 supernova = 0.2136
   (c) Fraction of binaries with 2 supernovae = 0.1648

### 4.2.1 Scatter plots as function of initial parameters

A. Find a useful / illustrative way to plot the outcomes of the binary evolution, in terms of the interactions experienced, as a function of the initial conditions.

1. Plot 1 : $M1_{ZAMS}$ vs $M2_{ZAMS}$
   Observations:
   (a) **Subplot 1, 4548 Unstable MTs** (counted binaries that undergo unstable MT events - they could also have undergone stable MT events) :
      i. Primary masses, $M1_{ZAMS}$ range from $0-140M_{\odot}$ and secondary masses, $M2_{ZAMS}$ range from $0-70M_{\odot}$.
      ii. It can be seen that there is a dense concentration of binaries at lower masses (both primary and secondary) - $M1_{ZAMS}, M2_{ZAMS} \in (0,40]M_{\odot}$.
      iii. Correlation between $M1_{ZAMS}$ and $M2_{ZAMS}$ is positive. There are a few points lying to the right of the $M1_{ZAMS} = M2_{ZAMS}$ line for higher values of $M1_{ZAMS}(> 80M_{\odot})$.
   (b) **Subplot 2, 1340 Stable MTs** (counted binaries that undergo only stable MTs, no unstable MTs) :
      i. Primary masses, $M1_{ZAMS}$ range from $0-150M_{\odot}$ and secondary masses, $M2_{ZAMS}$ range from $0-130M_{\odot}$. The range of masses here is greater than the ones for stable MT.

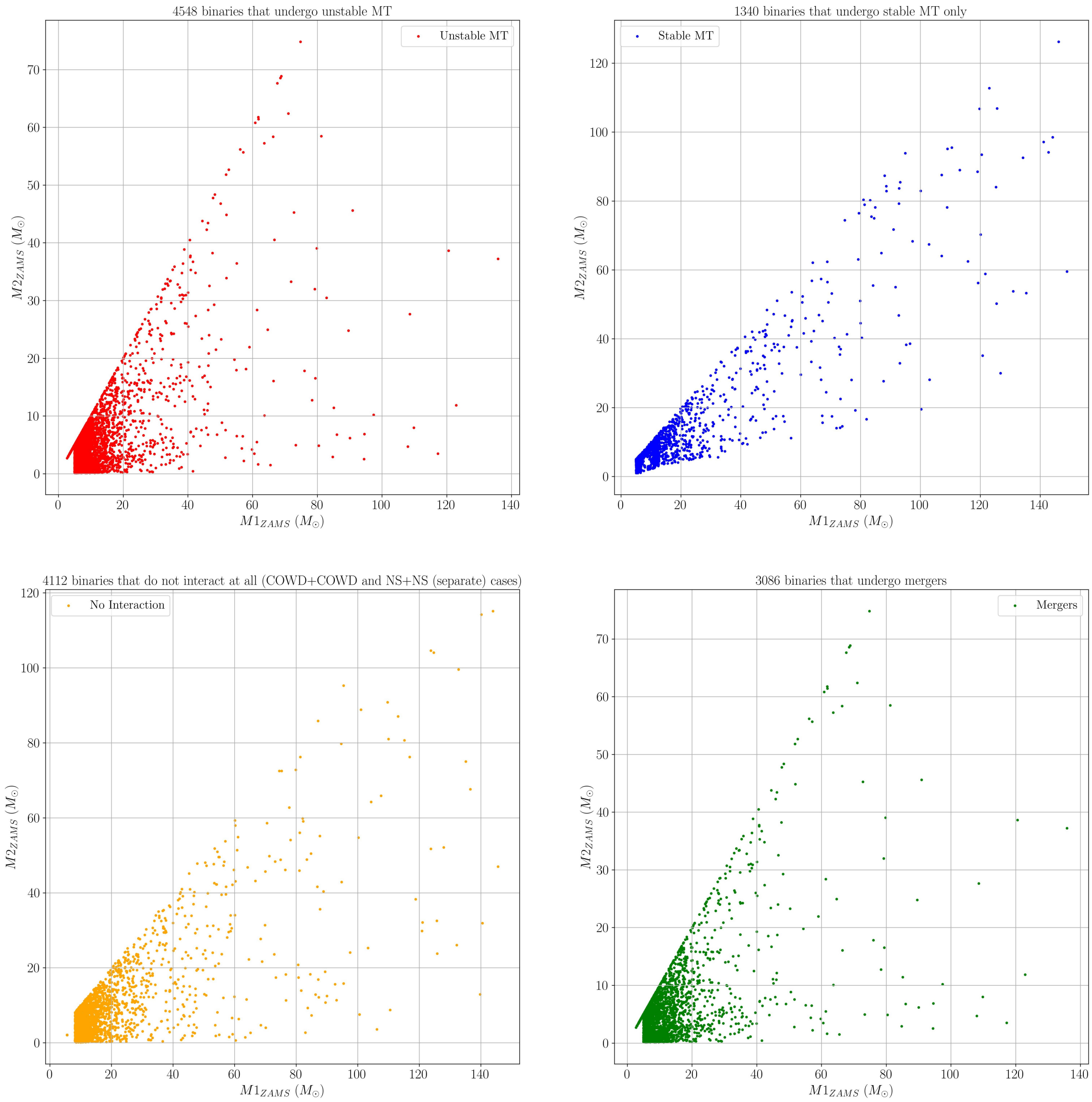


Figure 4.3: Scatter Plot of $M1_{ZAMS}$ vs $M2_{ZAMS}$ differentiating binaries that undergo **only** Stable MTs, binaries that undergo Unstable MTs, stellar mergers and binaries that have no interactions at all.

   ii. There is a similar trend of dense concentration at lower primary and secondary masses.
   iii. It can be seen that the distribution here is more densely concentrated/packed than compared to the unstable MT subplot. There is once again a positive correlation between $M1_{ZAMS}$ and $M2_{ZAMS}$ and is even more stronger (the correlation coefficient) than that of unstable MT case.
 (c) Subplot 3, **4112 binaries that do not interact** (counted binaries that do not have any MT events in their evolution time, so includes all COWD+COWD or NS+NS systems where each no RLOF events happened) :
   i. Similar distribution here as compared to the previous subplots. The range of primary and secondary masses is same as that for stable MT case.
   ii. Compared to stable MT plot, there is some distribution of binaries with higher $M1_{ZAMS}(> 60M_{\odot})$ and very lower $M2_{ZAMS}(< 10M_{\odot})$. This however, is absent in the stable MT plot.
 (d) **Subplot 4, 3086 binaries that undergo stellar mergers** (counted binaries that merge in Hubble time) :
   i. This plot contains data points that are almost 99 % the same as in the Unstable MT subplot. This indicates, almost all the 4548 binaries that undergo unstable MT, finally undergo stellar mergers. (If looked at closely, we can some data points that are in the red plot that are not in the green plot, such as near $(80,30)M_{\odot}$ ).

2. Plot 2 : $M1_{ZAMS}$ vs $SemiMajorAxis_{ZAMS}$
 Observations:
 (a) **Subplot 1, 4548 Unstable MTs** :
   i. Primary masses range from approximately $0-140M_{\odot}$ and Semi-major axis ranges from $0-25AU$ with one outlier at 175 AU.
   ii. For 99.99 % of binaries, the semi-major axis is very low (astronomically), not crossing 25 AU. From this, it can be inferred that in binaries that undergo unstable MTs, the semi-major axis is very low (around 10 AU), thus easily facilitating for a Common Envelope Evolution.
 (b) **Subplot 2, 1340 Stable MTs** :
   i. Primary masses range from approximately $0-140M_{\odot}$ and Semi-major axis ranges from $0-50AU$.
   ii. Compared to the previous plot, the distribution here is wide-spread, with stable MT taking place for distances > 20 AU.
 (c) Subplot 3, **4112 Binaries with no interactions** :
   i. Same range of primary masses as before, but there is a huge variation in the range of semi-major axis, it being $0-1000AU$.
   ii. Looking at the plot, obviously the data points are so widely distributed. Mainly, there is a dense concentration at lower masses, which correspond to the entire range of the semi-major axis.
 (d) **Subplot 4, 3086 Binaries that undergo stellar mergers** :
   i. Primary mass has the same range as before, but SemiMajorAxis ranges only form $0-16AU$. This is clearly shows that mergers happen at very close distances. Mergers are not very prone in binaries with large separations (there are very less binaries that merge as SMA

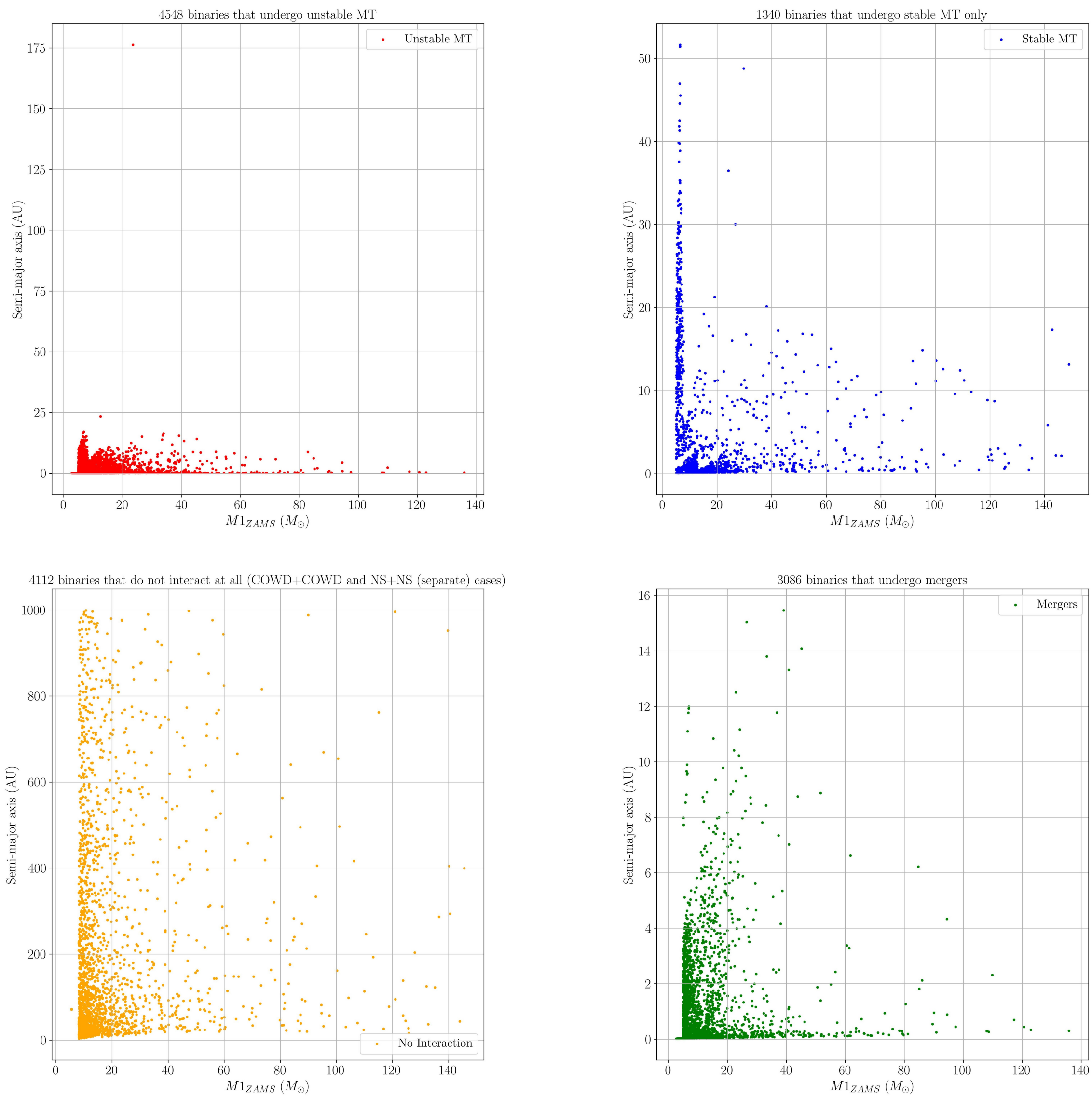


Figure 4.4: Scatter Plot of $M1_{ZAMS}$ vs $SMA_{ZAMS}$ differentiating binaries that undergo **only** Stable MTs, Unstable MTs, stellar mergers and binaries that have no interactions at all.

approaches 16 AU)

ii. There is a dense concentration of data-points at lower masses.

3. Plot 3 : $M2_{ZAMS}$ vs $SemiMajorAxis_{ZAMS}$

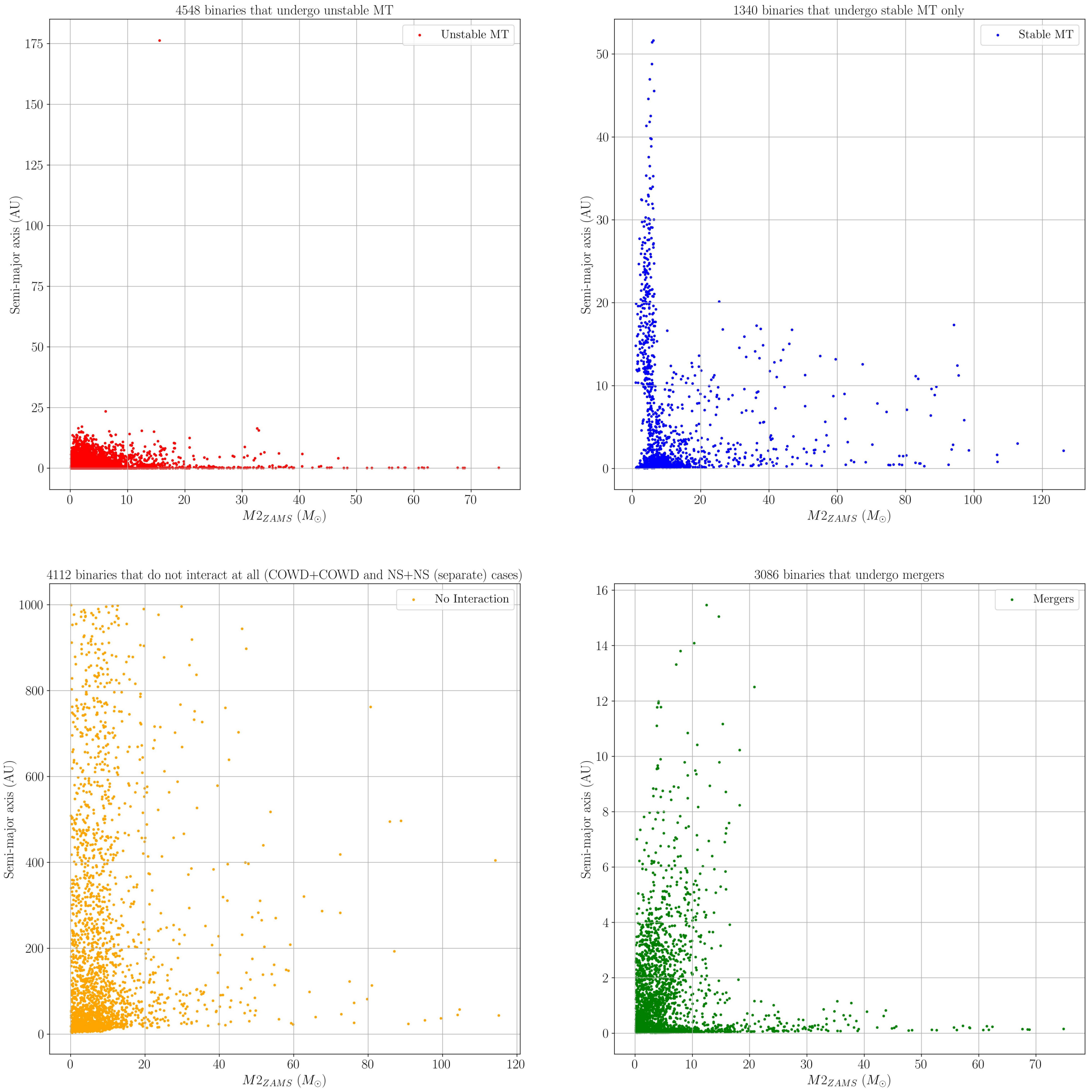


Figure 4.5: Scatter Plot of $M2_{ZAMS}$ vs $SMA_{ZAMS}$ differentiating binaries that undergo **only** Stable MTs, Unstable MTs, stellar mergers and binaries that have no interactions at all.

Observations:

(a) **Subplot 1, 4548 Unstable MTs** :

i. Similar to the unstable subplot (2a), the semi-major axis values are quite low, with the range being $0-25AU$. However, the range of masses ($M2_{ZAMS}$) is different from that of $M1_{ZAMS}$, with it being $0-100M_\odot$.

ii. There is dense concentration of data-points at lower masses with mostly all binaries lying below 25 AU. There are outlier points, some of which at around $(20M_\odot, 175AU)$ and $(96M_\odot, 0AU)$.

iii. The distribution again signifies that binaries with lower values of semi-major axes are more prone to undergo unstable MTs.

(b) **Subplot 2, 1340 Stable MTs** :

i. This subplot is very much similar to the previous Stable MT subplot (2b) for $M1_{ZAMS}$ vs $SemiMajorAxis_{ZAMS}$, except that the range of $M2_{ZAMS}$ is less than that of $M1_{ZAMS}$.

ii. There is a roughly semi-circular region - $M2_{ZAMS} \in (0,5]M_\odot$ and $SemiMajorAxis_{ZAMS} \in (0,10]AU$ where there are nearly no binaries present (except two or three.) This characteristic is not present in plot (ref: 2b).

(c) **Subplot 3, 4112 Binaries that do not interact** :

i. Again, this subplot is very much similar to the previous No interactions subplot (ref: 2c) for $M1_{ZAMS}$ vs $SemiMajorAxis_{ZAMS}$, but with one significant difference. It can be seen that there is a more denser concentration of binaries in the rectangular region $(0M_\odot, 0AU), (20M_\odot, 0AU), (20M_\odot, 1000AU), (0M_\odot, 1000AU)$ in here than compared to the other plot (ref: 2c).

(d) **Subplot 4, 3086 Binaries that undergo stellar mergers** :

i. Compared to the Stellar mergers subplot (ref: 2d) for $M1_{ZAMS}$ vs $SemiMajorAxis_{ZAMS}$, this plot is less scattered than the former.

ii. It is to be noted that majority of binaries with high secondary masses ($M2_ZAMS > 30M_\odot$) have so low semi-major axes (less than 1 AU). This number (of binaries) is much higher than compared to that in Stellar mergers subplot (ref: 2d) for $M1_{ZAMS}$ vs $SemiMajorAxis_{ZAMS}$.

### 4.2.2 Types of Supernovae experienced

Make a similar plot showing the outcomes in terms of number, and type of supernovae experienced.

According to COMPAS docs (ref: `https://compas.readthedocs.io/en/latest/pages/User%20guide/COMPAS%20output/standard-logfiles-record-specification-stellar.html#supernova-events-states`), there can be the following types of supernovae:

1. CCSN - Core Collapse Supernova
2. ECSN - Electron Capture Supernova
3. PISN - Pair Instability Supernova
4. PPISN - Pulsational Pair Instability Supernova
5. USSN - Ultra Stripped Supernova
6. AIC - Accretion-Induced Collapse
7. SNIA - Supernova Type Ia
8. HeSD - Helium-shell detonation

COMPAS denotes these types with numbers - 1 for CCSN, 2 for ECSN, 3 for PISN and so on. The COMPAS binary property is **SUPERNOVA_STATE**.

Now, from my analysis of the types of SN experienced by binaries for my run, I could only see CCSN and ECSN and no other type. So, the numbers are (each type differentiated into 1/2 Supernovae per binary):

1. CCSN : {'One SN':1950,'Two SN':1648}
2. ECSN : {'One SN':186,'Two SN':1648} (No, there is no mistake here. I got exactly

the same values for 'Two SN' in each CCSN and ECSN.)

Now, the plot (A stacked bar chart to show different types of Supernova experienced):

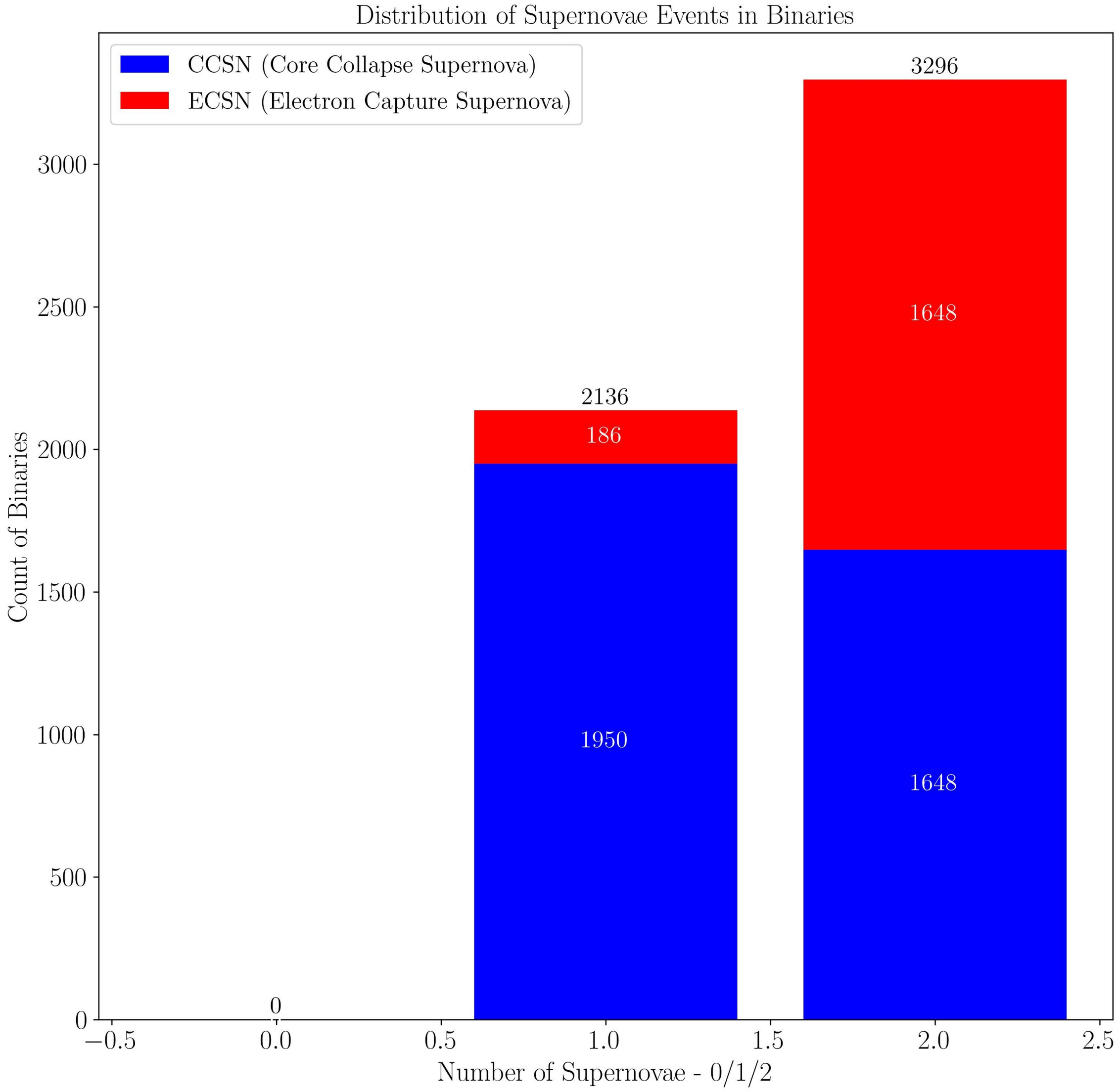


Figure 4.6: (Task-2) Supernovae classification by binaries that have 0/1/2 supernova events

## 4.3 Task 3

Repeat the 10,000 binary run, but with fully conservative mass transfer turned on again. How do the fractions of interacting and merging systems change? Are the initial conditions identical to the previous run? What could you do to make sure they are identical (i.e to make sure that the only differences come from the assumed physics)?

Comparing the results side-by-side,

| Statistics of simulation of 10,000 binaries | Task 2 | Task 3 |
|---|---|---|
| The time it took to record 10,000 binaries (CPU seconds) | 225.996 | 227.153 |
| Fraction of binaries that never interact | 0.4112 | 0.4108 |
| Fraction of binaries that experience unstable mass transfer | 0.4548 | 0.4848 |
| Fraction of binaries that experience stable mass transfer | 0.1340 | 0.1044 |
| Fraction of binaries that undergo stellar merger | 0.3086 | 0.3569 |
| Total number of supernovae | 5432 | 5652 |
| Fraction of binaries with 0 supernovae | 0.4567 | 0.4347 |
| Fraction of binaries with 1 supernova | 0.2136 | 0.2220 |
| Fraction of binaries with 2 supernovae | 0.3297 | 0.3433 |

Table 4.1: Summary of the tasks 2 and 3

1. The number of binaries that do not interact is nearly the same in both runs (just a difference of 4).
2. The number of mergers in Task 3 is higher than that in Task 2. This could be due to conservative mass transfer in Task 3 which could have influenced more number of mergers.
3. Number of binaries experiencing unstable MT is more in Task 3 than Task 2, while the number of binaries experiencing stable MT is more in Task 2 than compared to Task 3.
   This leads to the conclusion that in this circumstance, "conservative MT" likely leads to more unstable MTs.
4. However, the total number of binaries undergoing MT in both is nearly the same (5888 in task 2 and 5892 in task 3, again only a difference of 4).
5. In order to make sure that the initial conditions are identical, we can fix a 'random seed' for simulations (if suppose the random seed for Task-2 is '1718628379', then use this same seed for Task-3 as well using –random seed 1718628379 during execution of COMPAS).

### 4.3.1 Scatter plots as function of initial parameters

A. Find a useful / illustrative way to plot the outcomes of the binary evolution, in terms of the interactions experienced, as a function of the initial conditions.

Various interactions covered: Stable MT, Unstable MT, Mergers and No interactions

1. Plot 1 : $M1_{ZAMS}$ vs $M2_{ZAMS}$
   Observations:
   (a) **Subplot 1, 4848 Unstable MTs** (counted binaries that undergo unstable MT events - they could also have undergone stable MT events) :
      i. Primary masses, $M1_{ZAMS}$ range from $0-150M_{\odot}$ and secondary masses, $M2_{ZAMS}$ range from $0-140M_{\odot}$ (but, mostly tops at 120. There's an outlier data-point at about (140,140)).
      ii. It can be seen that there is a dense concentration of binaries at lower masses (both primary and secondary) - $M1_{ZAMS}, M2_{ZAMS} \in (0,40]M_{\odot}$.
      iii. Correlation between $M1_{ZAMS}$ and $M2_{ZAMS}$ is positive.
      iv. Compared to the same plot in task 2 (ref: 1a), the range of $M2_ZAMS$ is larger (extending upto 120 $M_{\odot}$ than just 70 $M_{\odot}$).
   (b) **Subplot 2, 1044 Stable MTs** (counted binaries that undergo only stable

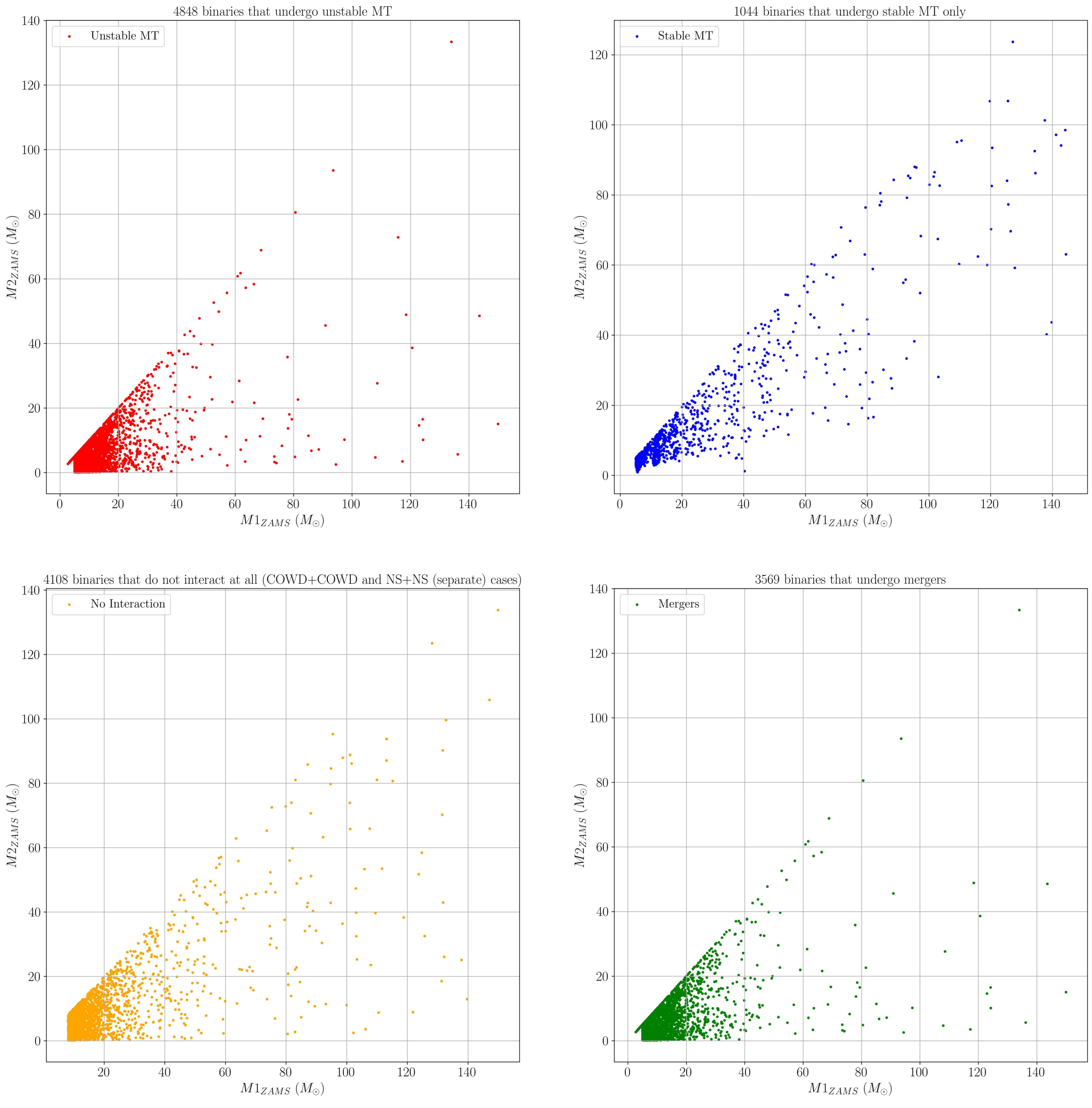


Figure 4.7: Scatter Plot of $M1_{ZAMS}$ vs $M2_{ZAMS}$ differentiating binaries that undergo **only** Stable MTs, binaries that undergo Unstable MTs, stellar mergers and binaries that have no interactions at all.

MTs, no unstable MTs) :

i. Primary masses, $M1_{ZAMS}$ range from $0-150M_{\odot}$ and secondary masses, $M2_{ZAMS}$ range from $0-130M_{\odot}$. We can see that the range of masses here is greater than the ones for stable MT.
ii. there is a similar trend of dense concentration at lower primary and secondary masses.
iii. It can be seen that the distribution here is more densely concentrated/packed than compared to the unstable MT subplot. There is once again a positive correlation between $M1_{ZAMS}$ and $M2_{ZAMS}$ and is even more stronger (the correlation coefficient) than that of unstable MT case.
iv. This plot is more or less the same, compared to the same plot in task 2 (ref: 1b).

(c) Subplot 3, **4108 binaries that do not interact** (counted binaries that do not have any MT events in their evolution time, so this includes all binaries that have become COWD+COWD or NS+NS (separate) systems without any MT events) :

i. Similar distribution here as compared to the previous subplots. The range of primary and secondary masses is same as that for stable MT case.
ii. Compared to stable MT plot, there is some distribution of binaries with higher $M1_{ZAMS}(>60M_{\odot})$ and very lower $M2_{ZAMS}(<10M_{\odot})$. This however, is absent in the stable MT plot. The same trend was also observed in the same plot for Task-2 (ref: 1c), which is more-or-less the same as this plot.

(d) Subplot 4, **3569 binaries that undergo stellar mergers** (counted binaries that merge in Hubble time) :

i. This plot contains data points that are almost 99 % the same as in the Unstable MT subplot. This indicates, almost all the 4848 binaries that undergo unstable MT, finally undergo stellar mergers.

ii. The same observation was also obtained for the same plot in task-2 (ref: 1d). The subtle differences that are present in the the plots is that the slope of line formed by the linear relation between $M1_{ZAMS}$ and $M2_{ZAMS}$ is greater in the task-2 plot than compared to this one, and the other being the number of stellar mergers.

**So, the differences between this plot and the same from task-2:**

i. Unstable MT (task-2,3): The slope of linear relation between $M1_{ZAMS}$ and $M2_{ZAMS}$ (the line like arrangement of points) is greater for Task-2 than Task-3.
ii. Stable MT (task-2,3): Both the plots are nearly the same, except for the difference in the number of data-points (i.e., different number of stable MTs in task-2 and 3).
iii. No Interactions (task-2,3): Same as that for Unstable MT - the slope of linear relation between $M1_{ZAMS}$ and $M2_{ZAMS}$ (the line like arrangement of points) is greater for Task-2 than Task-3.
iv. Stellar mergers (task-2,3): Same as that for stable MT - both the plots are nearly the same, except for the difference in the number of

data-points (i.e., different number of stable MTs in task-2 and 3).

2. Plot 2 : $M1_{ZAMS}$ vs $SemiMajorAxis_{ZAMS}$

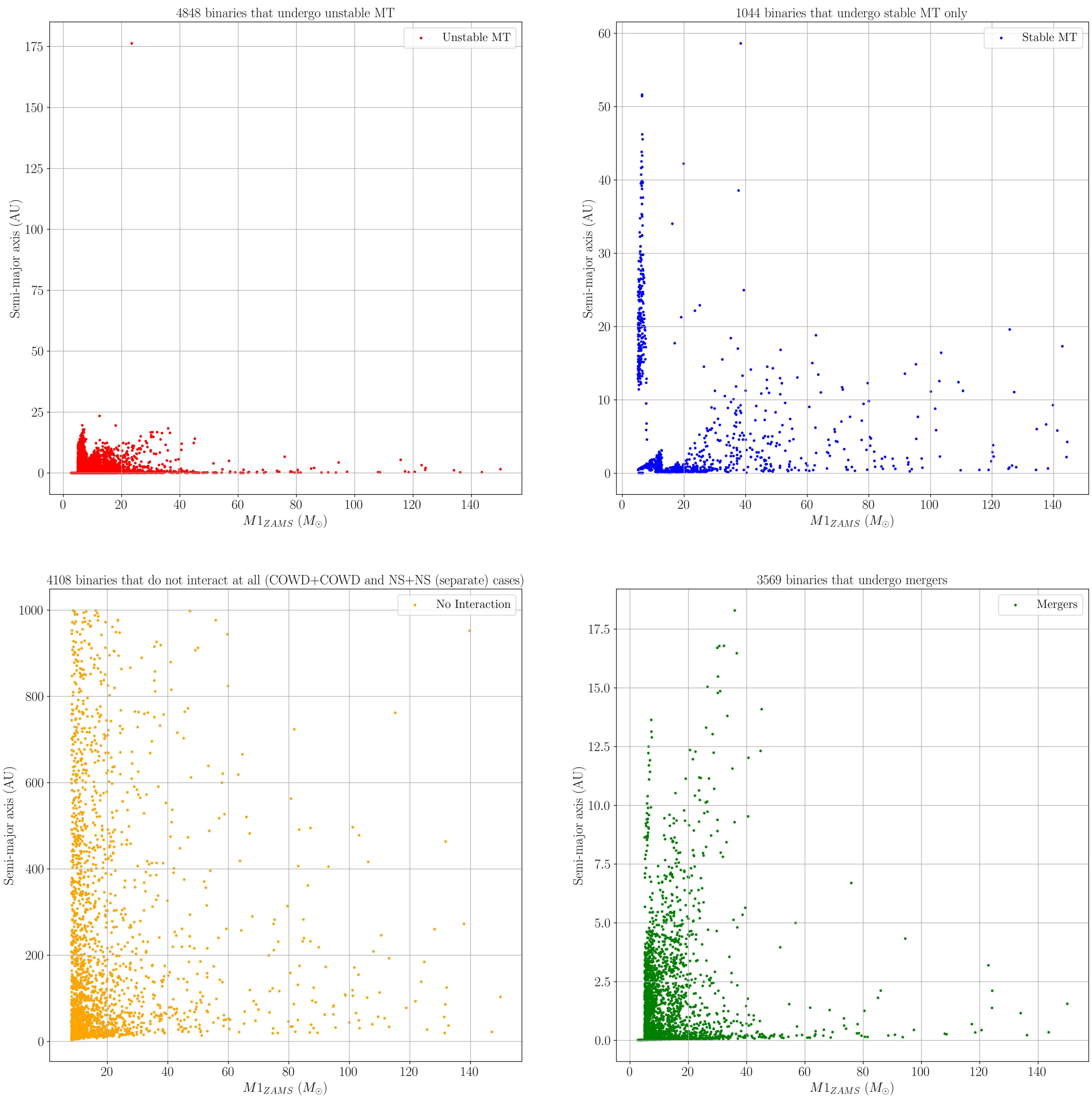


Figure 4.8: Scatter Plot of $M1_{ZAMS}$ vs $SMA_{ZAMS}$ differentiating binaries that undergo **only** Stable MTs, Unstable MTs, stellar mergers and binaries that have no interactions at all.

Observations:

(a) **Subplot 1, 4848 Unstable MTs** :
   i. Primary masses range from approximately $0-140M_{\odot}$ and Semi-major axis ranges from $0-25AU$ with one outlier at 175 AU.
   ii. For 99.99 % of binaries, the semi-major axis is very low (astronomically), not crossing 25 AU. From this, it can be inferred that in binaries that undergo unstable MTs, the semi-major axis is very low (around 10 AU), thus easily facilitating for a Common Envelope Evolution.

(b) **Subplot 2, 1044 Stable MTs** :
   i. Primary masses range from approximately $0-140M_{\odot}$ and Semi-major axis ranges from $0-50AU$.
   ii. Compared to the previous plot, the distribution here is wide-spread, with stable MT taking place for distances > 20, 30 AU.

(c) **Subplot 3, 4108 Binaries with no interactions** :
   i. Same range of primary masses as before, but there is a huge variation in the range of semi-major axis, it being $0-1000AU$.
   ii. Looking at the plot, obviously the data points are so widely distributed. Mainly, there is a dense concentration at lower masses, which correspond to the entire range of the semi-major axis.

(d) **Subplot 4, 3569 Binaries that undergo stellar mergers** :
   i. Primary mass has the same range as before, but SemiMajorAxis ranges only form $0-16AU$. This is clearly shows that mergers happen at very close distances. Mergers are not very prone in binaries with large separations (there are very less binaries that merge as SMA approaches 16 AU)
   ii. There is a dense concentration of data-points at lower masses.

### 4.3.2 Types of Supernovae experienced

| Make a similar plot showing the outcomes in terms of number, and type of supernovae experienced. |
|---|

Now, I have made a similar plot to what I had done in task-2, a stacked bar chart. In task-2, I had gotten only CCSN (Core Collapse Supernova) and ECSN ( Electron Capture Supernova), but here, I got CCSN, ECSN and **PISN (Pair Instability Supernova)**.
The numbers are:

1. CCSN : {'One SN': 1734, 'Two SN': 1716}
2. ECSN : {'One SN': 486, 'Two SN': 1715}
3. PISN : {'One SN': 0, 'Two SN': 1}

The plot, (once again, a stacked bar chart to differentiate between the types of supernovae) :

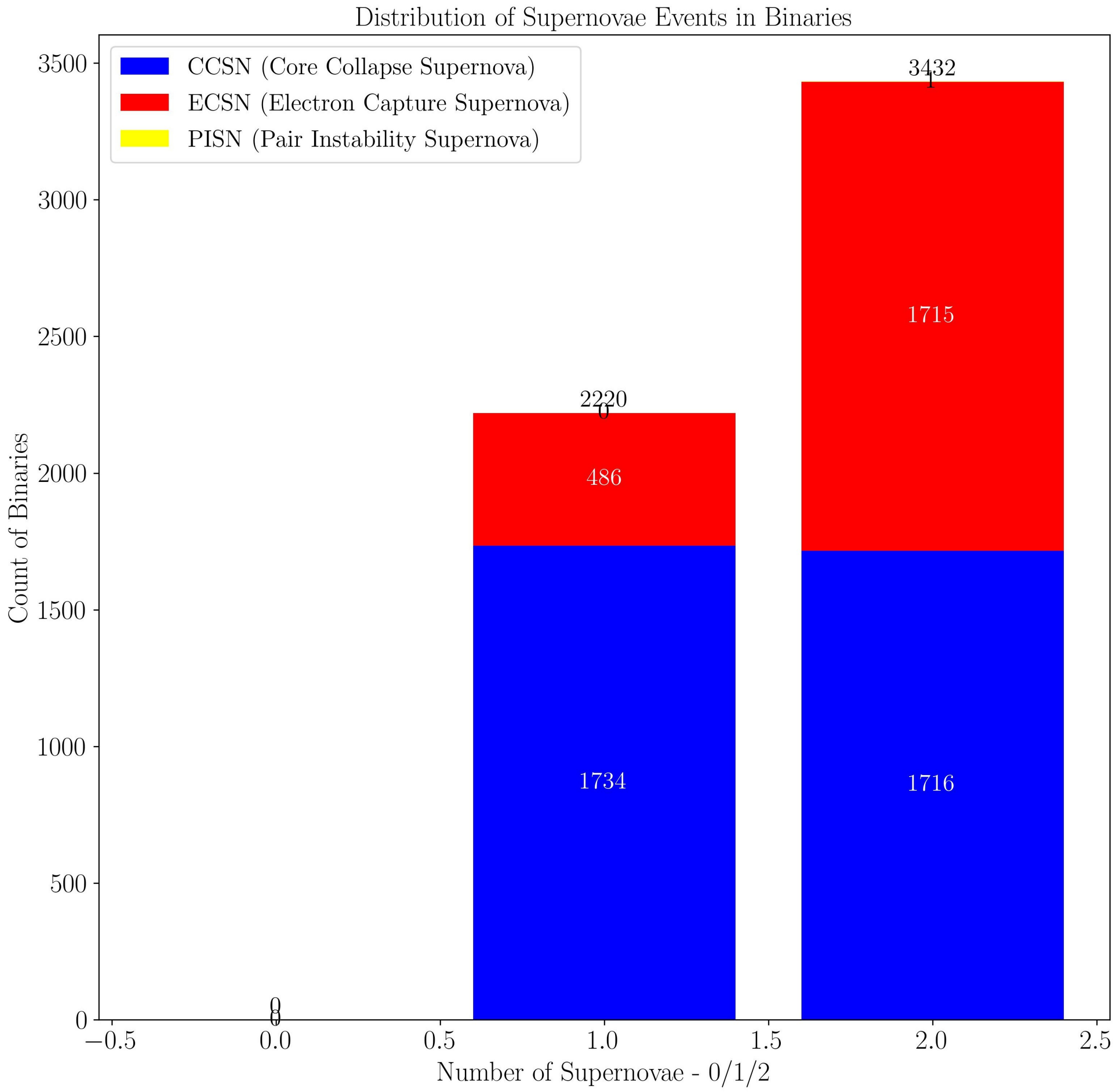


Figure 4.9: (Task-3) Supernovae classification by binaries that have 0/1/2 Supernova events

| Task Number | Supernova Type | Supernova Number (1/2) | Count of Binaries |
|---|---|---|---|
| Task 2 | CCSN | One SN | 1950 |
| Task 2 | CCSN | Two SN | 1648 |
| Task 2 | ECSN | One SN | 186 |
| Task 2 | ECSN | Two SN | 1648 |
| Task 3 | CCSN | One SN | 1734 |
| Task 3 | CCSN | Two SN | 1716 |
| Task 3 | ECSN | One SN | 486 |
| Task 3 | ECSN | One SN | 1715 |
| Task 3 | PISN | One SN | 0 |
| Task 3 | PISN | Two SN | 1 |

Table 4.2: Comparison of different types of SN experienced by binaries – Task-2 and 3

Explanations for the table of data:

1. Majority of the binaries (fraction = 0.6624 and 0.6104 of all SN events in task 2 and 3 respectively) undergo CCSN type SN events. It can be seen that total number of binaries that undergo CCSN is lesser in task-3 (3450) than compared to task-2 (3598).
2. Coming to one of the rarer SN events, Task-2 has 1834 binaries that undergo ECSN with 1648 out of 1834 binaries have both the stars undergo ECSN and the rest 186 where just one star in a binary undergoes ECSN. Task-3 has more number of binaries that undergo ECSN - 2201 than compared to task-2. This is also true for how many stars - either one or both undergo ECSN (486 > 186 and 1715 > 1648).
3. The rarest SN event, **PISN** occurs only in task-3 and that in only one binary where both the stars undergo PISN. The binary, 1718640009 has:
   (a) $M1_{ZAMS} = 49.537 M_{\odot}$ and $M2_{ZAMS} = 49.50348228051295 M_{\odot}$
   (b) $M1_{SN} = 13.26429562564192 M_{\odot}, M2_{SN} = 13.04885563668638 M_{\odot}$.

   It is known that PISN (Core Collapse caused by pair instability) occurs in stars that have $M_{SN} \in (140, 250) M_{\odot}$ (source: Wikipedia table). It is quite unheard of PISN occurring in such low mass binaries. **So, I think it might have occurred due to some noise in the COMPAS output.**
   (my COMPAS version at the time of running it: v02.50.01 – I re-ran the task after updating from v02.47.01 due to some bugs that I faced before; that's why all values for task2 and 3 are different from that in my mid-term report).

## 4.4 Task 0

(Task 0 is written after tasks 1,2 and 3 since I finished them in this order).

Run 10 binaries, with only fully-conservative mass transfer (i.e all mass that is lost by a donor star during an interaction is accreted onto the companion star - none is lost to the environment). Compare the initial and final masses of both stars in each binary. Is the sum the same at the beginning and the end? If not, why not?

The results obtained are:

| Binary Id | M1(ZAMS) | M2(ZAMS) | M1(final) | M2(final) | ZAMS-Total | Final-Total |
|---|---|---|---|---|---|---|
| 1719569454 | 5.878 | 1.603 | 1.313 | 0.623 | 7.481 | 1.936 |
| 1719569455 | 5.858 | 5.230 | 1.493 | 5.223 | 11.088 | 6.716 |
| 1719569456 | 6.033 | 0.150 | 1.154 | 0.150 | 6.183 | 1.304 |
| 1719569457 | 7.846 | 5.906 | 1.260 | 1.316 | 13.752 | 2.576 |
| 1719569458 | 5.770 | 5.770 | 5.770 | 5.770 | 11.540 | 11.54 |
| 1719569459 | 8.140 | 7.862 | 1.201 | 1.260 | 16.002 | 2.461 |
| 1719569460 | 9.267 | 7.941 | 1.234 | 1.457 | 17.208 | 2.691 |
| 1719569461 | 6.298 | 6.232 | 1.260 | 1.260 | 12.530 | 2.520 |
| 1719569462 | 5.129 | 1.518 | 1.085 | 0.695 | 6.647 | 1.780 |
| 1719569463 | 5.560 | 0.657 | 1.227 | 0.657 | 6.217 | 1.884 |

Table 4.3: Mass units in terms of solar mass ($M_{\odot}$). ZAMS - M1,M2 and final M1 and M2

1. **Binary 1719569454 :**

(a) There is no mass transfer event taking place in this binary. Each of the stars becomes a white dwarf.
(b) As expected, towards the end of its life (formation of a white dwarf), a star loses a lot of mass. Hence, star-1 goes from 5.878 $M_{\odot}$ at ZAMS to 1.3 $M_{\odot}$ while, star-2 goes from 1.603 $M_{\odot}$ at ZAMS to 0.623 $M_{\odot}$.
(c) Therefore, total mass at ZAMS $\neq$ total mass at the end.
(d) Further, there is also a double compact object merger taking place (at t=1.66e+21 Myr)

2. **Binary 1719569455 :**
   (a) Here, the stars undergo Common Envelope Evolution. Star-1 initiates a common envelope. It goes from 5.878 $M_{\odot}$ to 1.493 $M_{\odot}$. Whereas, mass of star-2 remains unchanged during this event. It can be concluded that the mass lost from star-1 is ejected out of the system (Even though FCMT is turned ON, this doesn't apply during CEE).
   (b) Hence, total mass at ZAMS $\neq$ total mass at the end.
   (c) At the end, there is a merger event of the two stars.

3. **Binary 1719569456 :**
   (a) Here too, the stars undergo Common Envelope Evolution. Star-1 being heavier, initiates the common envelope. Similar to the previous case, star-1 loses a lot of mass (which gets ejected out of the system) and ends up with 1.154 $M_{\odot}$ and star-2 remains unchanged (0.150 $M_{\odot}$ ).
   (b) Hence, total mass at ZAMS $\neq$ total mass at the end.
   (c) At the end, star-1 becomes a white dwarf, while star-2 still remains on MS.

4. **Binary 1719569457 :**
   (a) There is no MT event. So, obviously total mass at ZAMS $\neq$ total mass at the end of the stars' lives.
   (b) Anyways, star-1 undergoes a SN event to become a NS (7.85 $M_{\odot}$ at ZAMS to 1.3 $M_{\odot}$). While star-2 becomes a White Dwarf (5.9 $M_{\odot}$ at ZAMS to 1.3 $M_{\odot}$).

5. **Binary 1719569458 :**
   (a) Stellar Merger at the beginning. Star-1 and 2 both merge at ZAMS to form a bigger star on MS, which will undergo SSE on its own.
   (b) Hence, the total mass at ZAMS $\neq$ mass at the end.

6. **Binary 1719569459 :**
   (a) There is no MT event. Therefore, the total mass at the start cannot be equal to the total mass at the end - each of the stars begin to lose mass towards the end of their lives *due to stellar winds, etc.*
   (b) Star-1 undergoes supernova to become a neutron star. Some time later, star-2 also becomes a neutron star by undergoing a supernova explosion. Soon after, the orbit becomes unbound.

7. **Binary 1719569460 :**
   (a) Here, there is a stable MT from star-1 to star-2. This results in star-1 going from 9.198 $M_{\odot}$ to 1.929 $M_{\odot}$ and star-2 going from 7.910 $M_{\odot}$ to 15.110 $M_{\odot}$.

If we look here, **the total mass of the system before MT and after MT is the same** (approximately same, 17.108 $M_\odot$ and 17.039 $M_\odot$). Soon after, star-1 becomes a white dwarf (1.2 $M_\odot$).

(b) After a few Myrs, a CEE takes place. Initiated by star-2, it loses some mass to end up at 5.30 $M_\odot$. Then, it loses some more mass and undergoes a supernova to become a neutron star ($1.5 M_\odot$). At the end, the binary becomes unbound.

8. **Binary 1719569461 :**
   (a) No MT event here. Each of the stars in the binary evolve their own way and end up as neutron stars.
   (b) Special event: A double compact object (NS+NS) merger takes place.

9. **Binary 1719569462 :**
   (a) There's a stable MT from star-1 to 2. Star-1 goes from 1.7 $M_\odot$ to 1.1 $M_\odot$, while star-2 remains relatively unchanged at 1.5 $M_\odot$.
   (b) Towards the end, the system becomes a WD+WD binary (1.085 $M_\odot$ and 0.695 $M_\odot$).
10. **Binary 1719569463 :**
   (a) No MT event here. Each of the stars evolve separately while still being bound to each other gravitationally.
   (b) Star-1 being heavier, becomes a white dwarf first, while star-2 is still on MS.

## 4.5 Task 4

Run 100,000 binaries, in parallel. This can be done using a simple for loop in a bash script, creating background processes. If you don't know what this means, please reach out and we can help you get setup with this. If you have 10 free cores on your computer, you can run these 100,000 binaries in the amount of time it took you to run the 10,000 in the previous step. Verify that this is the case, and then combine the output files into one larger output. From this larger output file, how many Binary Black Holes do you produce? How many of these will merge in a Hubble time? How many Binary Neutron Stars, and how many Black Hole - Neutron Stars do you find, and how many of these merge within a Hubble time?

```
#!/bin/bash
j=$RANDOM
for (( i=1; i<=10; i++ ))
do
    ./COMPAS -c set-$i --random seed $j &
    j=$(($j+10000))
done
python3 ~/COMPAS/compas_python_utils/h5copy.py input set-1/set-1.h5
set-2/set-2.h5 set-3/3.h5 set-4/set-4.h5 set-5/set-5.h5 set-6/set-6.h5
set-7/set-7.h5 set-8/set-8.h5 set-9/set-9.h5 set-10/set-10.h5 -o Task-4-out.h5
```

- Script to run 100,000 binaries in parallel. Here, ten instances of the function run_compas() get called concurrently (i.e., they run at the same time) using the & operator. 10 new directories with names 1,2,3...10 are formed, each containing an hdf5 file named 1,2,3...10. Finally, I am appending all the 10 separate hdf5 files into one, named - *Task-4-out.h5*, which will contain data of the 100,000 binaries simulated.

- The computer on which the simulations were run had only 8 cores. So obviously, a bit more time would have taken to run them than compared to running 10,000 bianries.
  - For running 10,000 binaries, it took **225.996 CPU seconds**.
  - For running 10,000 binaries with Fully Conservative MT turned ON, it took **227.153 CPU seconds**.
  - For running 100,000 binaries in parallel, it took **CPU seconds**.

Now, coming to the results:

| Type | Total | Fraction |
|---|---|---|
| Double Compact Objects (DCOs) formed | 4286 | 0.04286 |
| Binary black holes formed | 3991 | 0.03991 |
| Black hole - Neutron star (BH-NS) binaries formed | 261 | 0.00261 |
| Neutron star binaries (NS-NS) formed | 34 | 0.00034 |
| Number of Binary black holes that merge in a Hubble time | 334 | 0.00334 |
| Number of Black Hole - Neutron stars that merge in a Hubble time | 121 | 0.00121 |
| Number of Neutron star binaries that merge in a Hubble time | 26 | 0.00026 |

Table 4.4: Data extracted from BSE_Double_Compact_Objects

### 4.5.1 Binary Black Holes

Observations:

**Histograms of primary, secondary, chirp masses and mass ratios**

I am comparing the results obtained with what has been concluded from Mandel and Farmer's paper (2) :

1. It can be seen that masses of the companions stars of merging BBHs predominantly between 5 - 20 MSun, while those belonging to non-merging BBHs fall majorly in the range 2 - 30 MSun.
2. Merging black hole binaries have lower chirp masses compared to black hole binaries that don't merge.
3. According to Mandel and Farmer (2), the individual black holes masses span from $\simeq 2.6M_\odot$ to $\simeq 80M_\odot$. It can be seen that this is indeed true for all the 3991 BBHs.
4. Again, according to the paper (2), the vast majority of merging binary black holes, have both companion stars below $45M_\odot$. It can been seen from the plots that all of the companion (primary and secondary) stars have masses less than 45 MSun.
5. Most observed merging binary black holes are consistent with having equal mass components, i.e., majority of the merging BBHs have mass ratios around 1 (from Mandel and Farmer) From my plot, nearly 140-170 binaries have mass ratios in the range of 0.5 to 1 and about a 100 in the range 1 to 1.5 and the rest from 1.5 to 4. There are no merging BBHs that have mass ratios more 4.

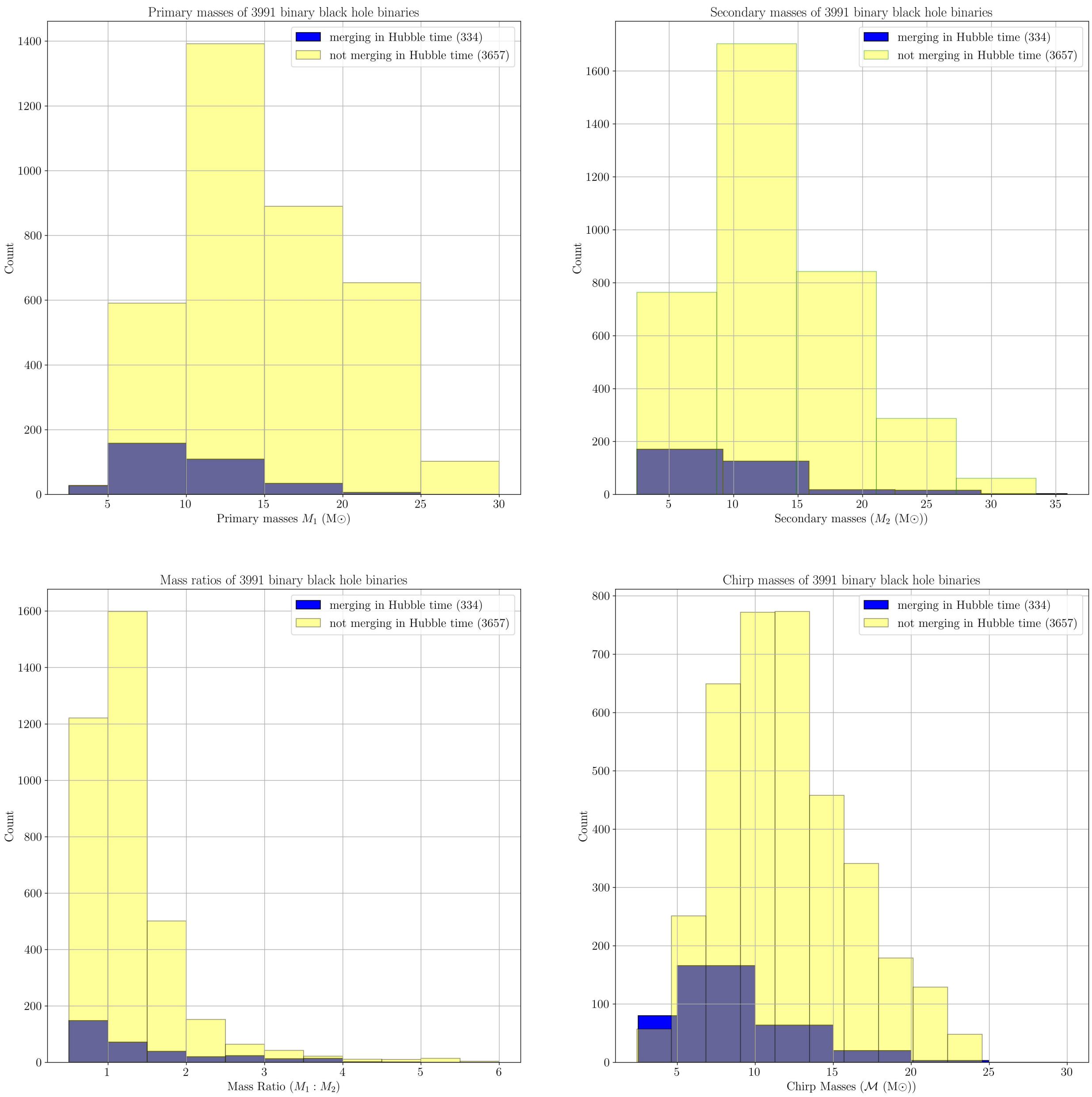


Figure 4.10: Histograms of various parameters of BBHs

6. The mass ratios of most merging black-hole binaries produced through the isolated binary evolution channel are likely to be on the equal side of 2 : 1.

**Plotting initial parameters $\in$ Mass@ZAMS(1), Mass@ZAMS(2), Semi-Major Axis@ZAMS**

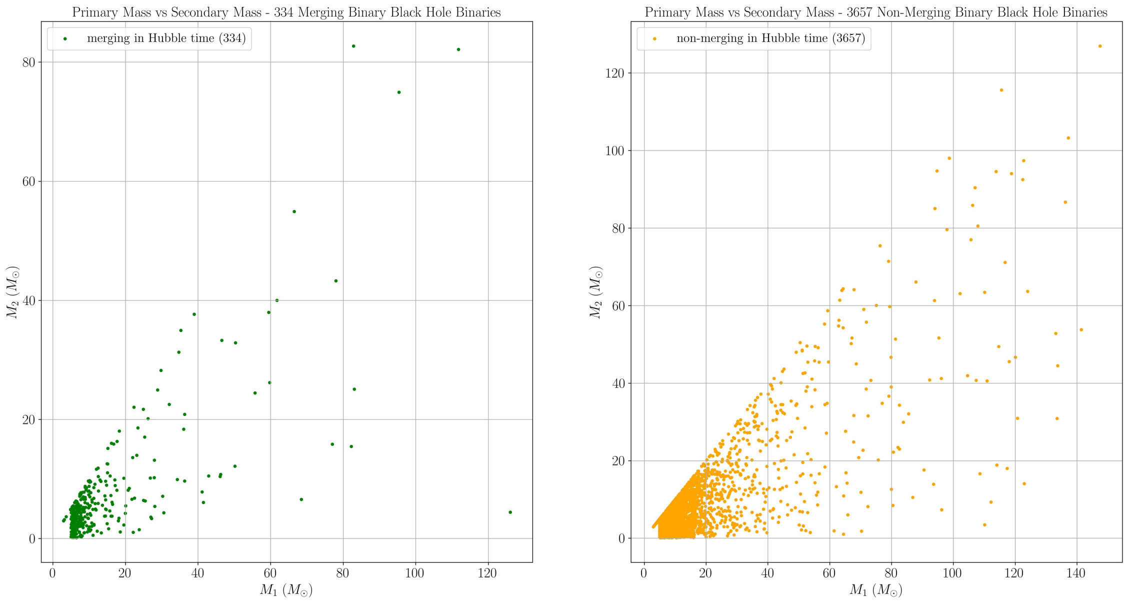


Figure 4.11: Scatter plots differentiating merging and non-merging BBHs

Observations:

1. Merging BH-NS:
   (a) The distribution of masses is more concentrated at lower masses, particularly below $M_1$ and $M_2$ of $20M_\odot$.
   (b) There are a few outliers with higher masses, indicating some systems with one or both black holes having masses up to around $80-120M_\odot$.
   (c) The overall trend shows a correlation where higher primary masses often correspond to higher secondary masses, but there is a wide spread.
2. Non-Merging BH-NS:
   (a) The distribution of masses extends over a larger range, particularly up to higher primary and secondary masses compared to the merging systems.
   (b) There is a higher density of systems with low primary and secondary masses, but the spread is broader across both axes.
   (c) Systems with higher primary masses also tend to have higher secondary masses, similar to the merging systems, but there are many more such pairs.

### 4.5.2 Black Hole - Neutron Stars

**Histograms of primary, secondary, chirp masses and mass ratios**

Observations from the plot:

1. (Plot: Primary masses of *BH-NSs*) The primary masses of BH-NS mostly belong to that of the stars that would eventually become black holes. Most of the merging ones belong to mass category of 2.5 - 10 $M_\odot$, while, the non-merging ones are concentrated between 5 - 12 $M_\odot$.

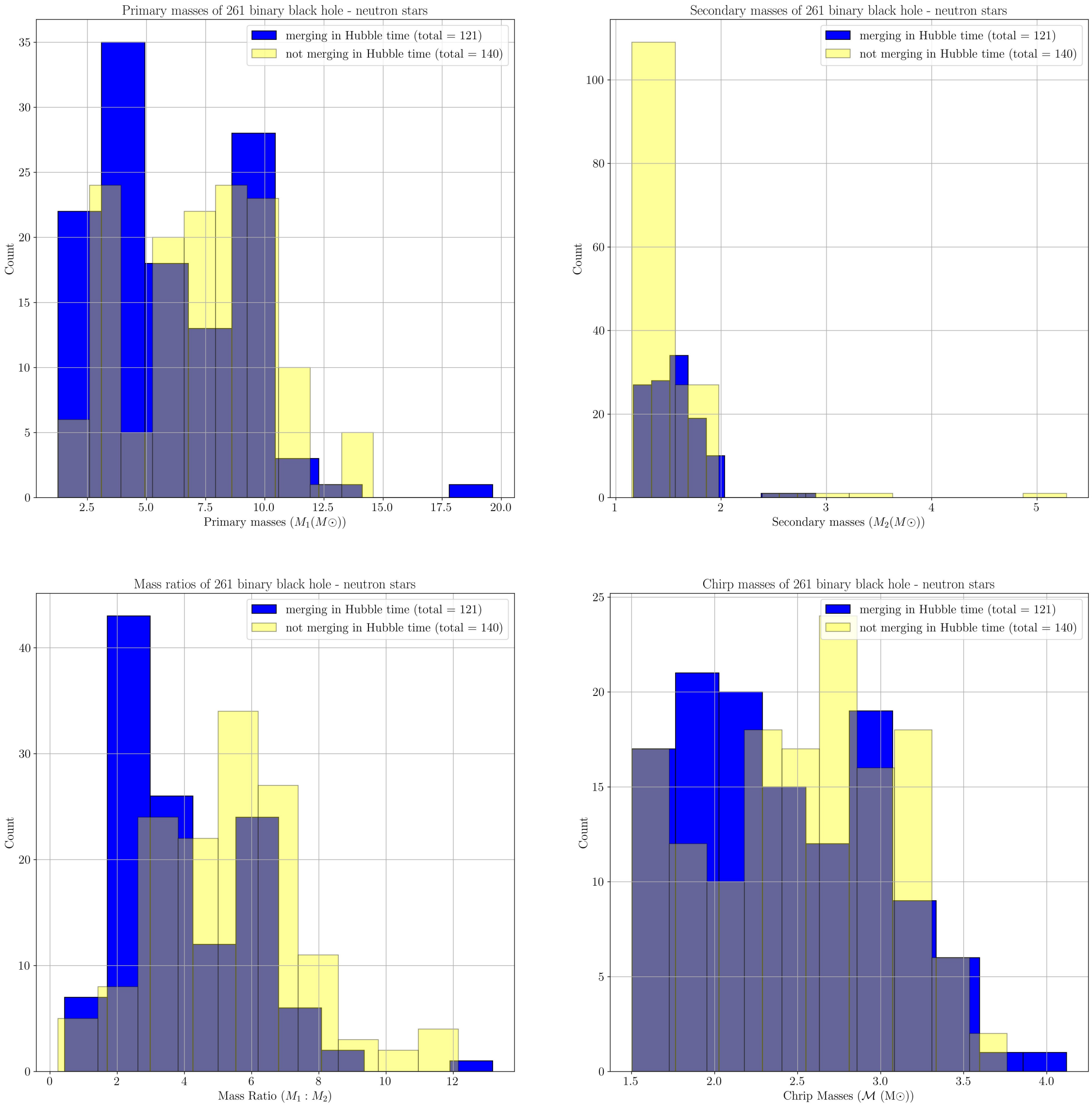


Figure 4.12: Histograms of various parameters of *BH-NS*s

2. (Plot: Secondary masses of *BH-NSs*) This plot is completely different from the previous one. This is evident from the fact the secondary masses in BH-NS systems belong to Neutron stars.
   (a) The non-merging ones are concentrated between 1.4 - 2 $M_\odot$, with the majority under 1.5 $M_\odot$.
   (b) The merging ones are roughly uniformly distributed between 1.4 - 2 $M_\odot$.
3. (Plot: Mass ratios of *BH-NSs*) Here,
   (a) for the merging ones, the mass ratios follow a skew right uni-modal distribution , with maximum number of binaries falling between mass ratios of 2:1 and 4:1.
   (b) The non-merging binaries have a roughly normal distribution, with maximum binaries having mass ratios between 5:1 to 7:1.
4. (Plot: Chirp masses of *BH-NSs*) Here, the merging BH-NS systems have a skewed-left distribution while the non-merging ones have a skewed-right distribution of chirp masses. Very less binaries (< 10) have chirp masses greater than 3.5 $M_\odot$.

**Plotting initial parameters $\in$ Mass@ZAMS(1), Mass@ZAMS(2), Semi-Major Axis@ZAMS**

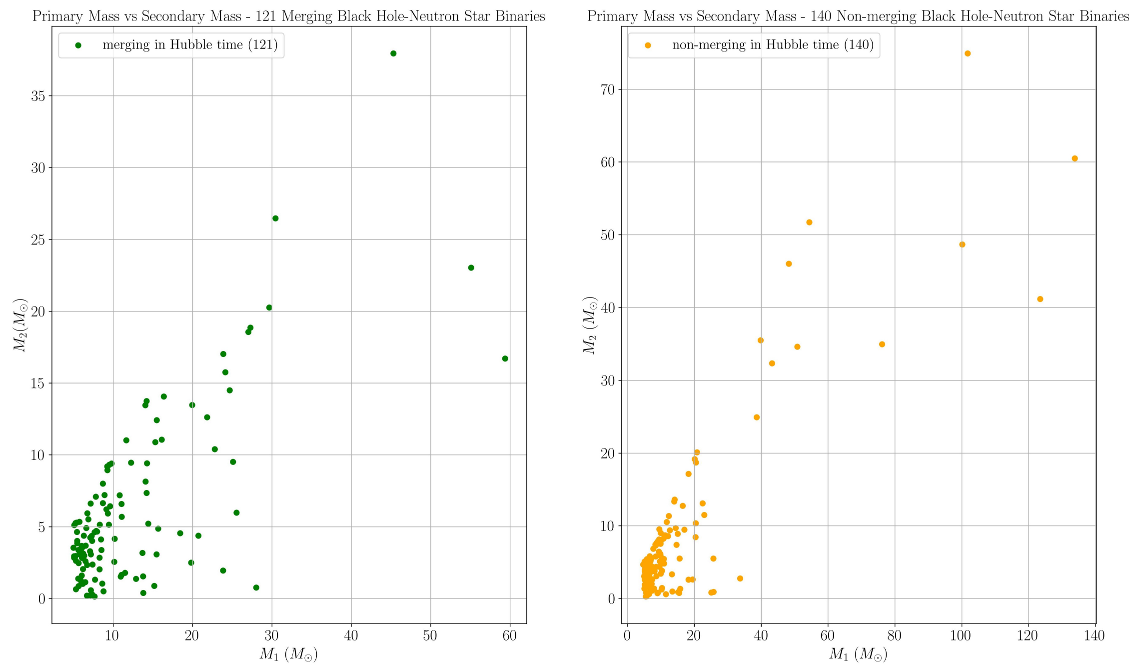


Figure 4.13: Scatter plots differentiating merging and non-merging BH-NSs

Observations:
1. Merging BH-NS:
   (a) The plot is more concentrated at lower masses, and it can be seen for $M_1, M_2 \in [0, 10] M_\odot$, most merging binaries are found here.
   (b) There are very few binaries that have $M_2 > 20 M_\odot$
   (c) The overall trend shows a correlation where higher primary masses often correspond to higher secondary masses, but with fewer high mass pairs compared to the non-merging systems.
2. Non-Merging BH-NS:
   (a) There is a significant concentration for $M_1, M_2 \in [0, 20] M_\odot$.

(b) There is a wider distribution at higher masses ($M_1, M_2 > 30M_\odot$) than compared to merging ones.

### 4.5.3 Binary Neutron Stars

**Histograms of primary, secondary, chirp masses and mass ratios**

The set of 100,000 binaries that I ran, only generated 34 binary neutron stars (NS-NS) with 26 merging in Hubble time and the other 8 not merging.

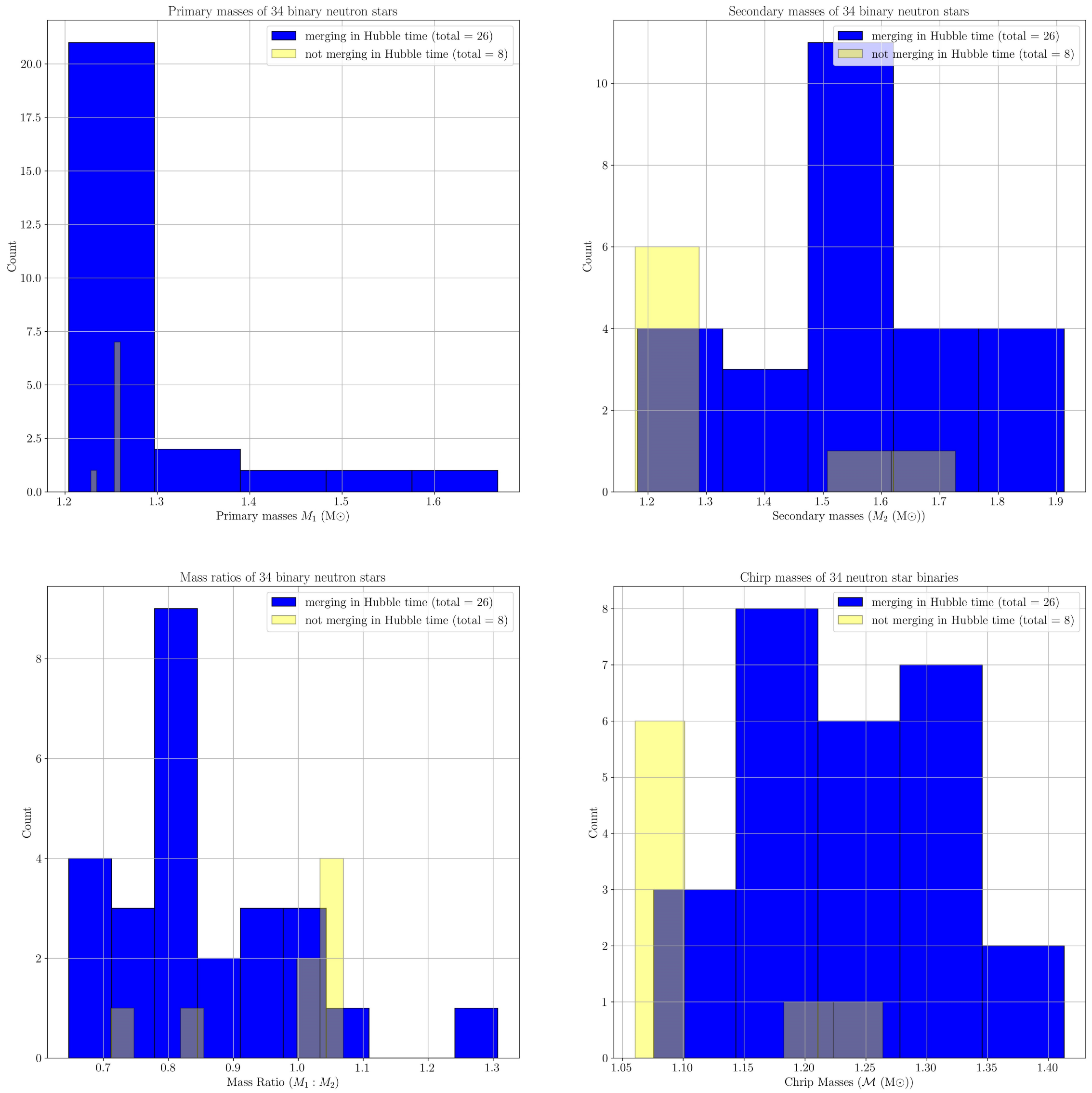


Figure 4.14: Histograms of various parameters of *BNS*s

Observations from the plot:

1. (Plot: Primary masses of *BNS*s)
   (a) In this plot, for **merging** NS-NS binaries, 21 stars have masses in the range 1.2 - 1.3 $M_\odot$, 2 between 1.3 to 1.4 $M_\odot$ and 3 between 1.4 to 1.7 $M_\odot$.
   (b) For **non-merging** NS-NS binaries, 1 star has mass closer (slightly greater) to 1.2 $M_\odot$ while the remaining 7, each have the same mass, which is closer (slightly lesser) to 1.3 $M_\odot$.

2. (Plot: Secondary masses of *BNS*s)
   This plot is the complete opposite of the previous one.
   (a) **Merging ones:** Follows a roughly normal, uni-modal distribution. Mode of 11 for stars having masses in the range 1.5 - 1.6 $M_\odot$.
   (b) **Non-merging ones:** 6 stars have masses between 1.2 - 1.3 $M_\odot$ and the other 2 between 1.5 - 1.75 $M_\odot$.
3. (Plot: Mass ratios of *BNS*s)
   (a) Most number (9) of merging BNSs have mass ratios around 0.8. This can be justified from the previous 2 plots $\Rightarrow$ Primary masses were on an average lower than secondary masses.
   (b) Coming to non-merging ones, the mode and average mass ratio of these binaries is around 1.0 .
4. (Plot: CHirp masses of *BNS*s)
   (a) **Merging BNSs:** There are 21 binaries having chirp masses between 1.15 - 1.35 $M_\odot$, 3 around 1.1 $M_\odot$ and 2 between 1.35 to 1.40 $M_\odot$.
   (b) **Non-merging BNSs:** Majority (6) of the binaries have chirp masses between 1.05 - 1.10 $M_\odot$ and the rest (2) around 1.20 $M_\odot$.

**Plotting initial parameters $\in$ Mass@ZAMS(1), Mass@ZAMS(2)**

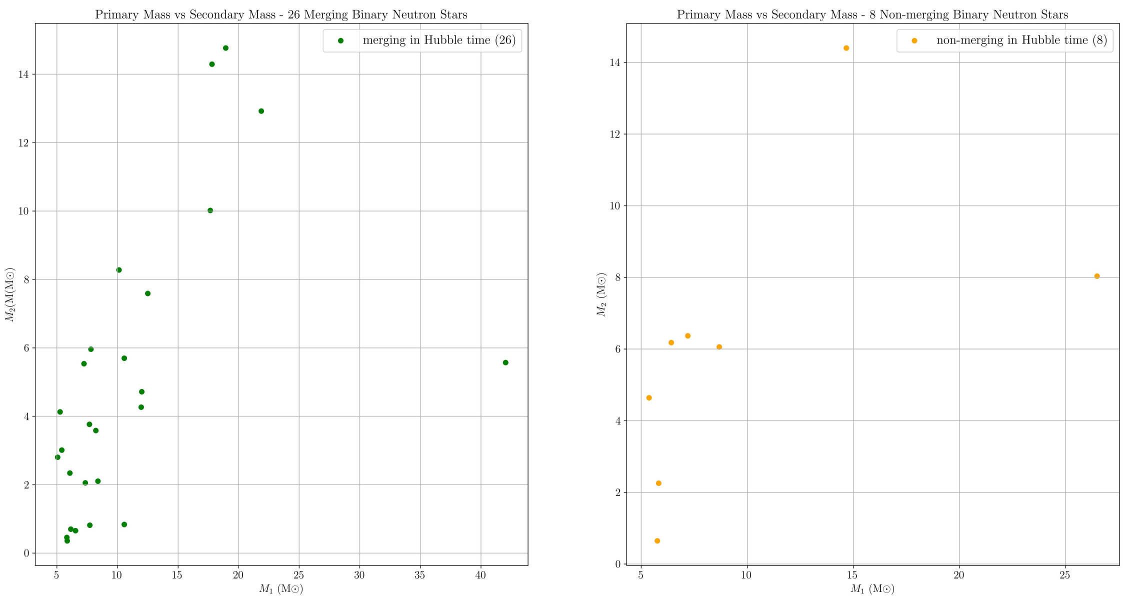


Figure 4.15: Scatter plots differentiating merging and non-merging BNS systems

Observations:
1. Here we can see that primary masses at ZAMS are in general greater than (or, greater than or equal to) secondary masses at ZAMS (this is in fact the definition of primary and secondary masses)
2. Merging BNS:
   (a) We can see that primary masses in general lie between $[5, 25)M_\odot$ and secondary masses between $(0, 15)M_\odot$.
   (b) There is a positive correlation here - as primary mass increases, secondary mass also increases and vice versa.
3. Non-Merging BNS:
   (a) $M_1 \in [5, 28)M_\odot$ and $M_2 \in (0, 15]M_\odot$ but, most of $M_2$ is found below 8 $M_\odot$.

(b) There are fewer data points, hence nothing more can be said, but the distribution shows a similar trend where higher primary masses correlate with higher secondary masses.

### 4.5.4 Plots of Compact Object binaries as a functions of their initial parameters

Initial parameters that were used: (from BSE_System_Parameters of the HDF5 file)

1. Mass@ZAMS(1)
2. Mass@ZAMS(2)
3. SemiMajorAxis@ZAMS

- ***Plot 1 -*** $M1_{ZAMS}$ **vs** $M2_{ZAMS}$

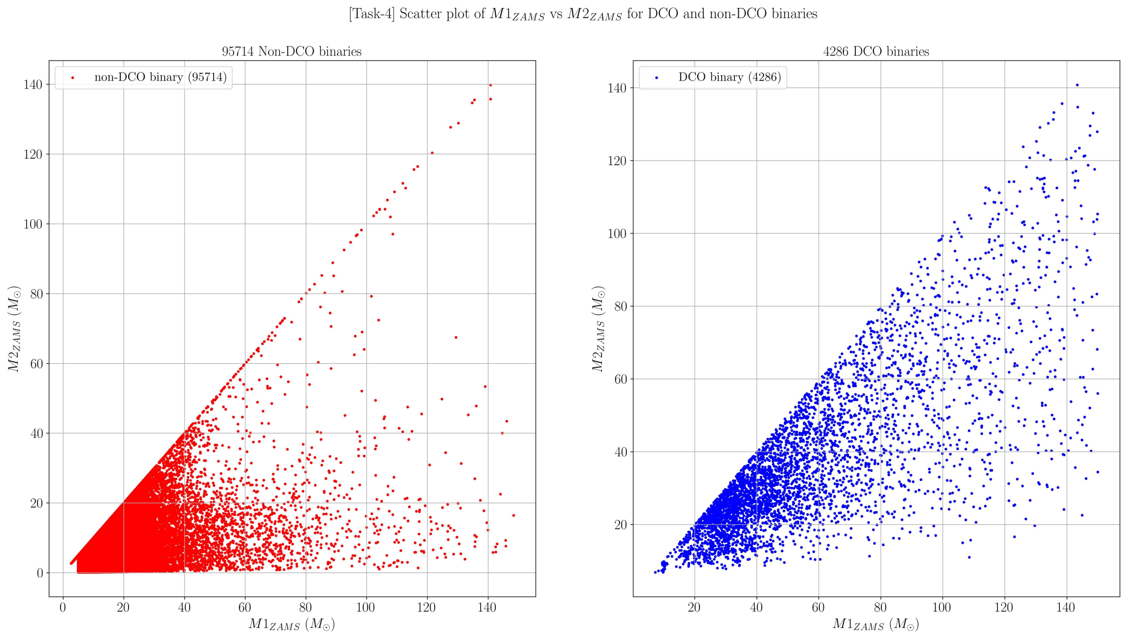


Figure 4.16: Scatter plot of $M1_{ZAMS}$ vs $M2_{ZAMS}$, differentiating DCOs and non-DCO binaries

- Observations:
  1. Non-DCO binaries:
     (a) The primary masses range from $0-150M_\odot$ and the secondary masses from $0-140M_\odot$ .
     (b) The data points form a dense triangular distribution with most points lying below $M1_{ZAMS} = 100M_\odot$ and $M2_{ZAMS} = 80M_\odot$.
     (c) The distribution shows an unclear correlation where higher primary masses not always correspond to higher secondary masses. There is a significant spread, especially at lower masses.
     (d) As $M1_{ZAMS}$ increases, the density of number of binaries which have higher $M2_{ZAMS}$ , decreases. This is evident from the empty region inside the triangular distribution.
     (e) There's very loose clustering around the $M1_{ZAMS} = M2_{ZAMS}$ line.
  2. DCO binaries:
     (a) The primary masses range from $0-150M_\odot$ and the secondary masses from $0-141M_\odot$.

   (b) The distribution forms a more densely packed triangular shape compared to non-DCO binaries.
   (c) The correlation between primary and secondary masses is more pronounced in DCO binaries, with fewer outliers and a denser clustering around the $M1_{ZAMS} = M2_{ZAMS}$ line.
3. DCO binaries have fewer outliers and a more consistent mass relationship than compared to non-DCO ones.
4. The stronger mass correlation in DCO binaries likely reflects the need for certain mass ratios to facilitate the formation of double compact objects.

- ***Plot 2 -*** $M1_{ZAMS}$ ***vs*** $SMA_{ZAMS}$ ***and*** $M2_{ZAMS}$ ***vs*** $SMA_{ZAMS}$

  Observations:
- $M1_{ZAMS}$ vs $SMA_{ZAMS}$
  1. Non-DCO binaries -
     (a) $M1_{ZAMS} \in (0, 150)M_{\odot}$ and $SMA_{ZAMS} \in (0, 1000]AU$
     (b) There is dense clustering at lower primary masses, for all ranges of SMA.
     (c) As, the mass increases, the SMA tends to decrease (the rough hyperbolic outline that can be seen).
  2. DCO binaries -
     (a) This plot has a scattered distribution. Compared to the previous plot, there is dense clustering occurring at lower SMA.
     (b) For primary masses < 20 $M_{\odot}$, the SMA remains in under 200 AU (some 6-7 binaries with M1 < 20 have SMA > 200), while for masses greater than 200, the distribution of SMA is anywhere between 0 - 1000 AU.
- $M2_{ZAMS}$ vs $SMA_{ZAMS}$
  1. Non-DCO binaries -
     (a) This plot is less scattered than compared to $M1_{ZAMS}$ vs $SMA_{ZAMS}$ Non-DCO binaries. Again, there is dense clustering at lower masses ($M2_{ZAMS} < 30M_{\odot}$).
     (b) Correlation between $M2_{ZAMS}$ and $SMA_{ZAMS}$ is negative and much more pronounced that then other plot.
  2. DCO binaries -
     (a) This plot is pretty similar to $M1_{ZAMS}$ vs $SMA_{ZAMS}$ DCO binaries.
     (b) It can be seen that there are lesser number of binaries with secondary masses > 100 $M_{\odot}$ at higher SMA values (>600 AU).

## 4.6 Task 5

Run 1,000,000 binaries (of course, in parallel). Try to vary the parameters of the simulation such as to match the chirp mass distribution of merging BBHs as close to the chirp distribution of the 70 merging BBHs obtained during the LIGO O3 run. There is no right answer/ right plot.

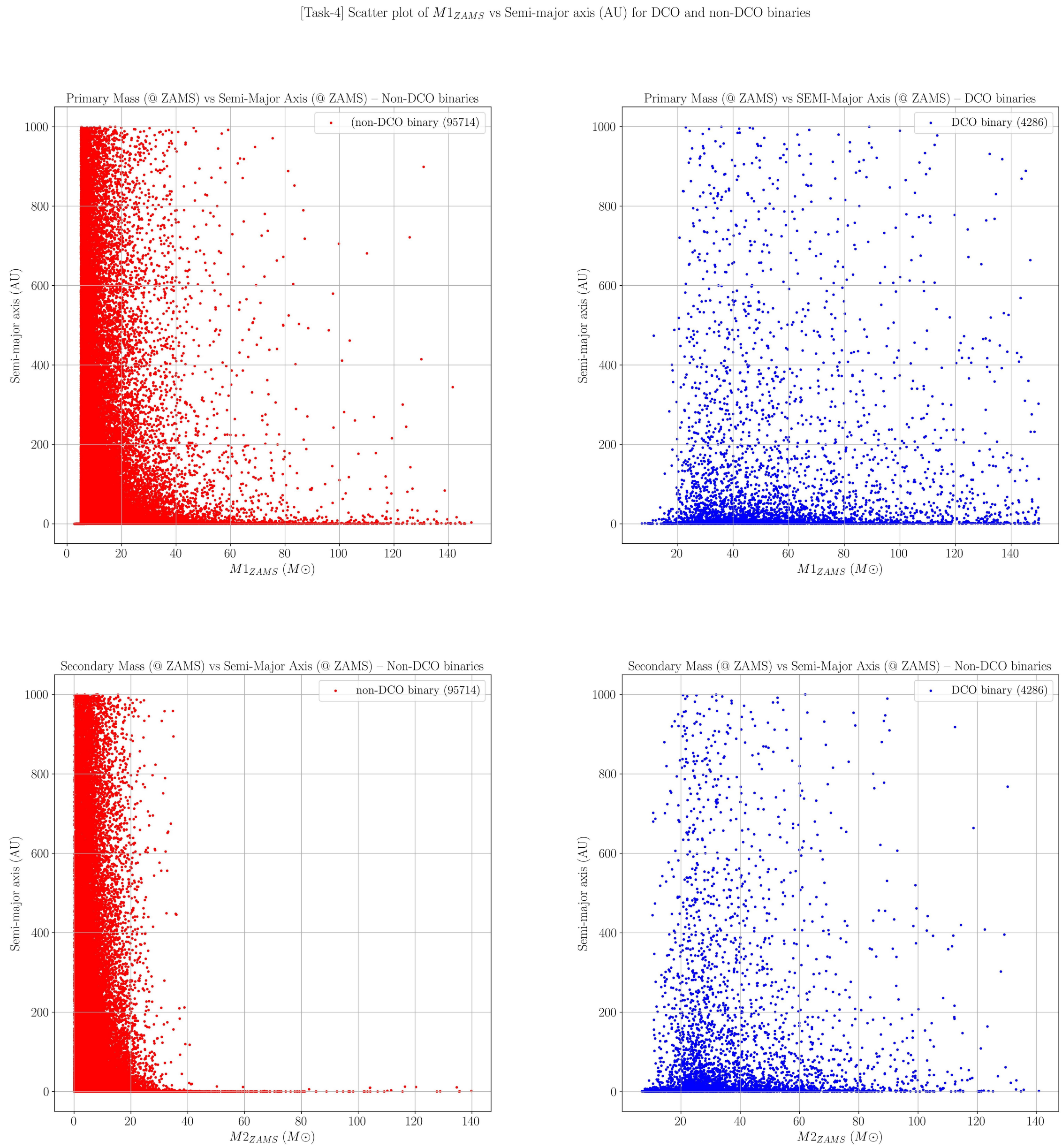


Figure 4.17: Scatter plot of $M1_{ZAMS}$ vs SemiMajorAxis@ZAMS and $M2_{ZAMS}$ vs SemiMajorAxis@ZAMS, for DCO and Non-DCO binaries

### 4.6.1 LIGO O3

The LIGO O3 data has recorded 76 merging DCOs. (ref: References,4)

1. The different DCOs:
   (a) 69 BBHs
   (b) 4 NS-BHs
   (c) 2 BNSs
   (d) 1 BBH or BH-NS (the paper - 4 has classified it as a BBH, so 70 BBHs overall)
2. Stats:
   (a) The mode of the data lies between $(20, 30)M_{\odot}$.
   (b) Mean of chirp masses = 24.150 $M_{\odot}$.
   (c) Standard Deviation = 12.250 $M_{\odot}$.

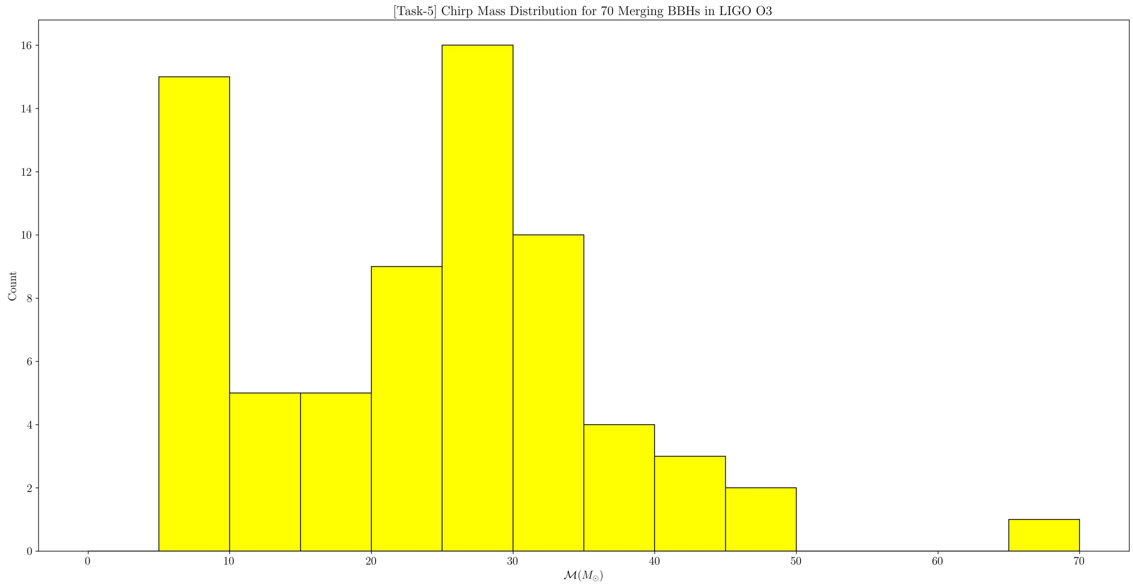


Figure 4.18: LIGO O3 - Histogram

### 4.6.2 Runs

**Note** : All of the runs use the same set of random seeds - starting at 11040 and ending at 1011040. So, it can be assured that only the same set of binaries are simulated again and again, but with different parameters. Further, I modified the script written for Task-4 such that I added a nested for loop in place of a single for loop. This however didn't increase the efficiency compared to a single for loop (10 times 10 times 10,000 binaries VS 10 times 100,000 binaries). Anyways, the script is as follows:

```
# Run-1
#!/bin/bash
j=11040 # 11040 is the random seed - that I started with for run 1 and
# used it for all subsequent runs
for (( i=1; i<=10; i++ ))
do
    for (( p=1; p<=10; p++ ))
    do
            ./COMPAS --random-seed $j -n 10000 -c set-$i$p -o ./data-one
            -million-binaries/run-test/ &
            #echo $j
            j=$((j+10000))
    done
    j=$((j+1))
done
# At the end, I had to combine all the HDF5 files generated into one
# single HDF5 file using the h5copy.py included in the COMPAS/src/ directory
```

**Run-1 (default parameters)**

1. It can be seen that the chirp mass average is lower (17.223 $M_\odot$) compared to the LIGO run (24.150 $M_\odot$). Likewise, the standard deviation (3.359 $M_\odot$) too is

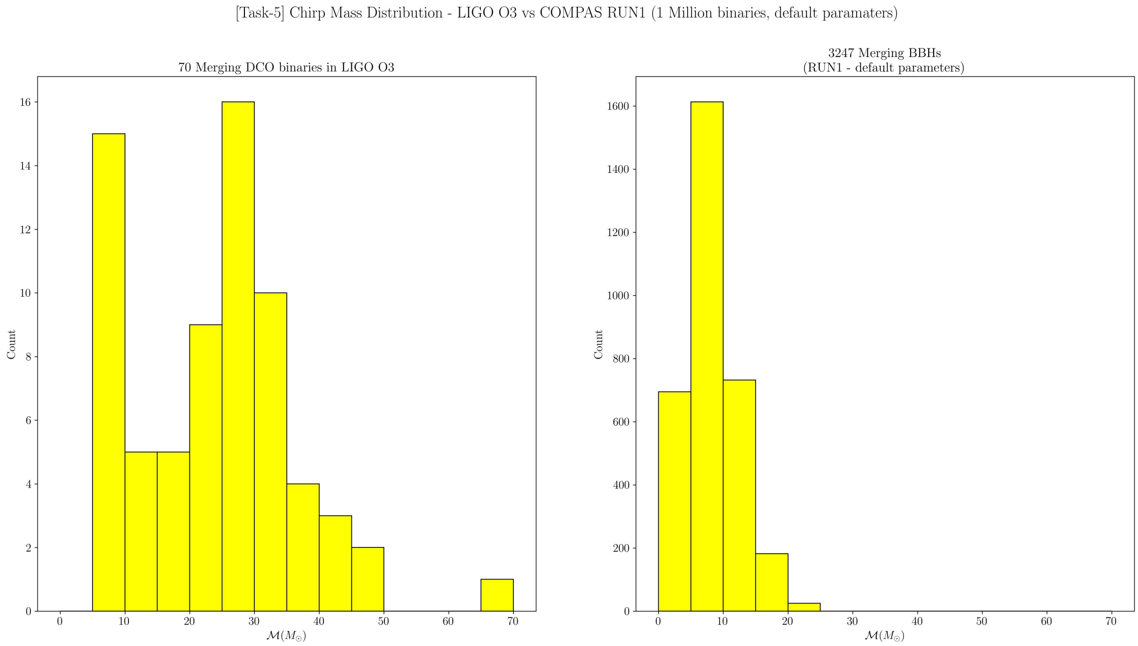


Figure 4.19: Chirp mass distribution - LIGO vs Run-1 (Default parameters)

| Events and parameters | Stats |
|---|---|
| Merging DCOs | 4623 |
| **Merging BBHs** | **3247** |
| Merging BH-NSs | 1131 |
| Merging BNSs | 245 |
| Mean of chirp masses of merging BBHs | 17.223 $M_\odot$ |
| Standard Deviation of chirp masses of merging BBHs | 3.359 $M_\odot$ |
| Mode of masses of merging BBHs | $\in [5,10] M_\odot$ |

Table 4.5: Summary of Run-1 Details

lower compared to the the LIGO run (12.250 $M_\odot$).

2. In order to vary the distribution so as to closely match the LIGO run, I tried to :
   (a) **Shift the plot towards the right (the peaks)**, i.e., increase the average of the chirp masses of the BBHs.
   (Since the chirp mass is related to the individual masses $M_1$ and $M_2$ by the relation: $\mathscr{M} = \frac{(M_1.M_2)^{0.6}}{(M_1+M_2)^{0.2}}$, ($M_1$ and $M_2$ are the masses of the compact objects) varying the parameters such that the ***initial-mass-min*** and ***initial-mass-max*** could help increase the average of the chirp mass distribution and help achieve something closer to the actual LIGO distribution.)
   (b) **Increase the spread of the plot**. After increasing the masses by using constraints on minimum limit of masses, I got plots where the range of chirp masses actually decreased (this of course happens since chirp mass increases with increasing individual masses). In addition, I didn't get any BBHs with very high chirp masses ($\mathscr{M} > 40 M_\odot$), in fact nothing beyond 30 (even for runs that had - " –initial-mass-min 90.0 –secondary-mass-min 10.0").
   (c) In addition, I also tried changing the **metallicity**. I kept the metallicity

for each of the binaries near to the default minimum (0.0001). I noticed the average mass increasing once I made this change (specifically, I ran 2 runs each having the same initial mass constraints - one with the metallicity constraint and another without it).

**Run-2 (constraints on the initial masses of stars)**

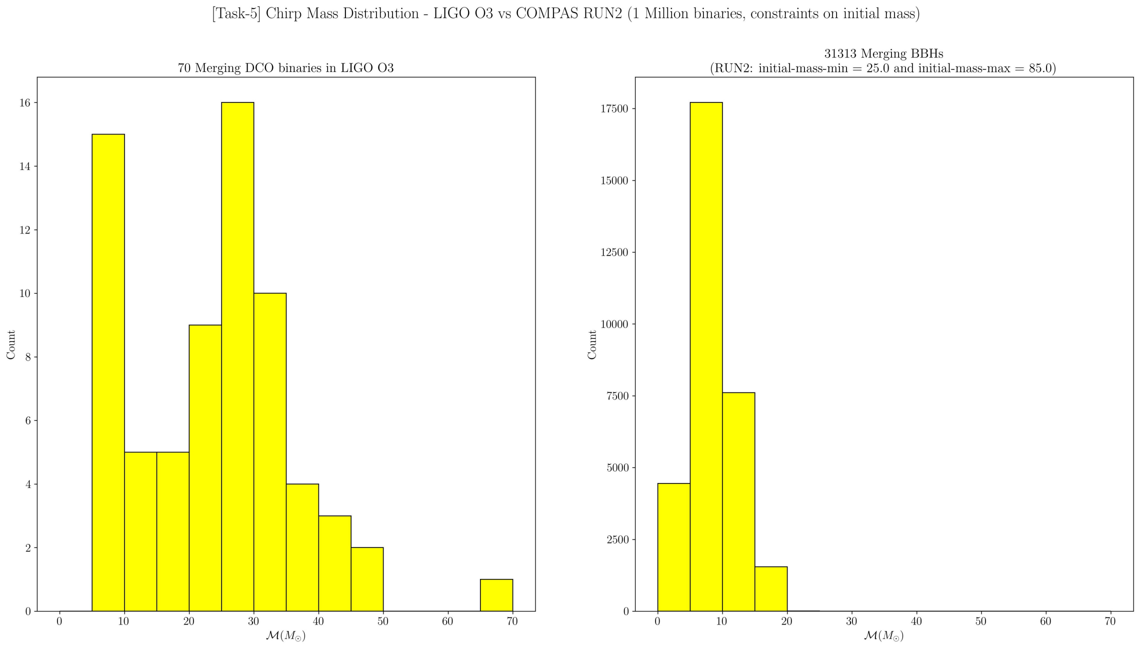


Figure 4.20: Run-2

1. Parameters changed:
   (a) *initial-mass-min* : Changed the value from 5.0 (default) to 25.0 $M_\odot$.
   (b) *initial-mass-max* : Changed the value from 150.0 (default) to 85.0 $M_\odot$.

| Events and parameters | Stats |
|---|---|
| Merging DCOs | 38476 |
| **Merging BBHs** | **31313** |
| Merging BH-NSs | 17851 |
| Merging BNSs | 0 |
| Mean of chirp masses of merging BBHs | 8.713 $M_\odot$ |
| Standard Deviation of chirp masses of merging BBHs | 3.227 $M_\odot$ |
| Mode of masses of merging BBHs | $\in [5, 10] M_\odot$ |

Table 4.6: Summary of Run-2 Details

2. In this run, I basically tried to find out how the distribution of chirp masses changed when I increased the minimum mass limit to 5 times the original value and decreased the maximum mass limit to 85 from 150 $M_\odot$. Of course with this constraint, there would predominant number of formations of BBHs, followed by BH-NSs and there wouldn't be any formation of BNSs.
3. What I found out is that (pertaining to chirp masses of merging BBHs only),
   (a) There cannot be any BBHs found beyond 20 $M_\odot$.

(b) 55.9 % of merging BBHs have chirp masses in the range of $[5, 10]M_{\odot}$, 23.9 % have chirp masses in the range of $[10, 15]M_{\odot}$.

(c) Compared to Run-1, the range of chirp masses decreased. There are zero BBHs in the range $[20, 25]M_{\odot}$ for Run-2, whereas, Run-1 has quite a sizable number in this mass range.

**Conclusion** : So, I realized that I have to increase the *initial-mass-min* and *initial-mass-max* even more .

### Run-3 (constraints on mass parameters - modified)

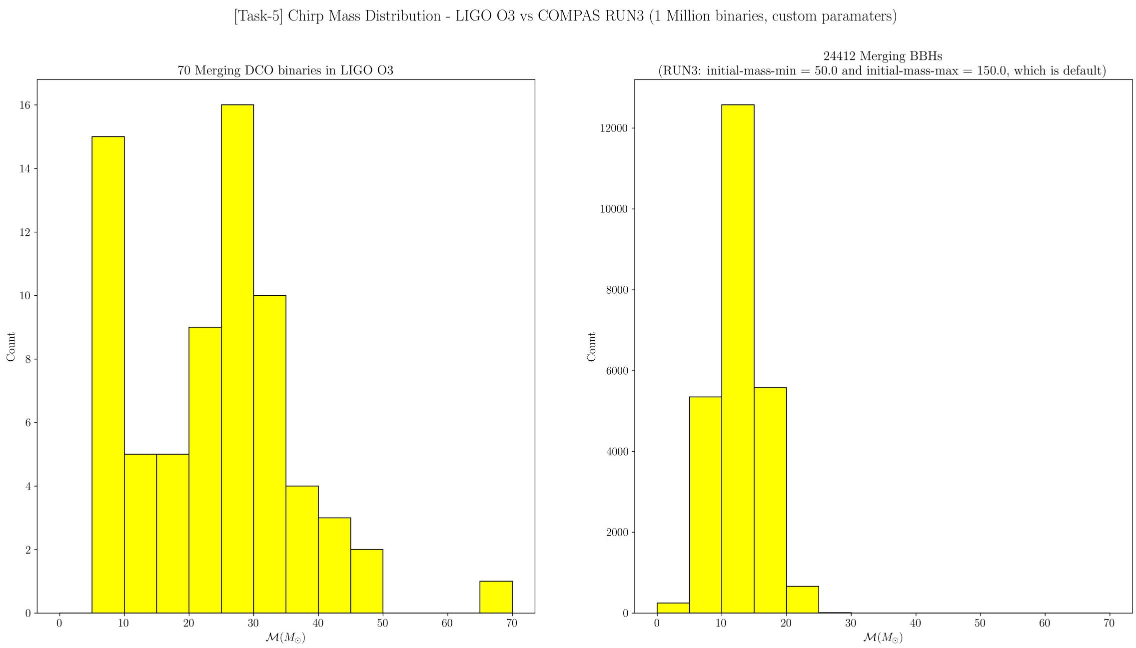


Figure 4.21: Run-3

1. Parameters changed:
   (a) *initial-mass-min* : Changed the value from 5.0 (default) to 50.0 $M_{\odot}$.

| Events and parameters | Stats |
|---|---|
| Merging DCOs | 25241 |
| **Merging BBHs** | **24412** |
| Merging BH-NSs | 829 |
| Merging BNSs | 0 |
| Mean of chirp masses of merging BBHs | 12.699 $M_{\odot}$ |
| Standard Deviation of chirp masses of merging BBHs | 3.753 $M_{\odot}$ |
| Mode of masses of merging BBHs | $\in [10, 15]M_{\odot}$ |

Table 4.7: Summary of Run-3 Details

2. Just as thought about in the conclusion of Run-2, the plot has shifted towards right compared to Run-2's plot. The average has increased and so has the mode of the distribution. The spread has also gotten a bit better with merging

BBHs found in $[20,25]M_{\odot}$.

In the next plot, I will try changing the metallicity parameter without changing the already altered parameter (initial-mass-min, which was set to 50.0) of this run and notice changes.

**Run-4 (Constrains on mass and metallicity parameters)**

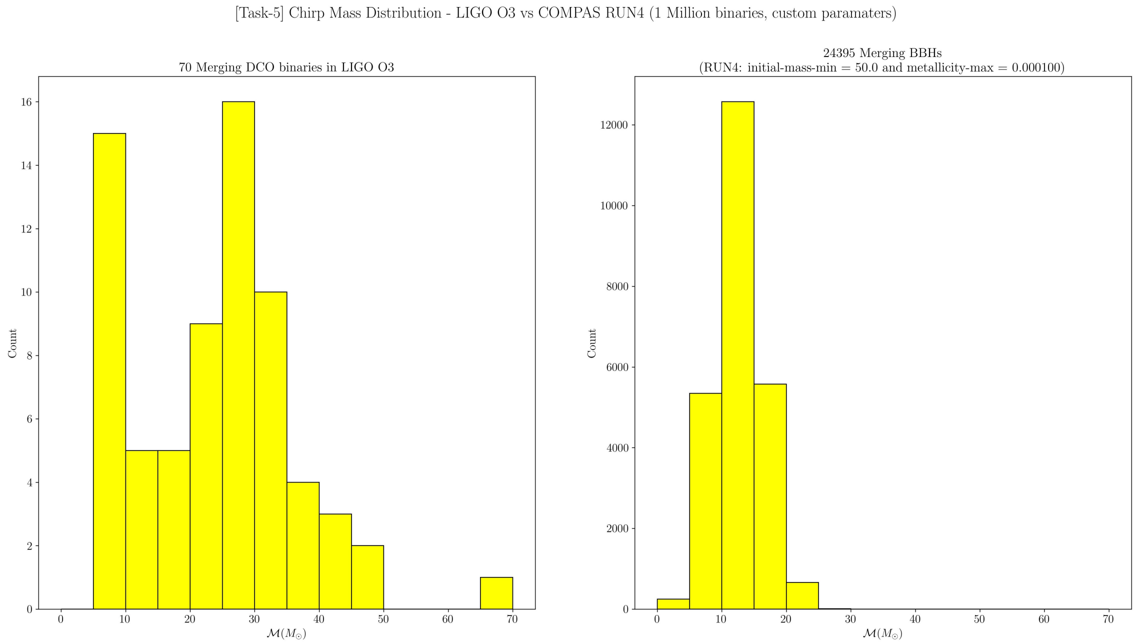


Figure 4.22: Run-4

1. Parameters changed:
   (a) *initial-mass-min* : Changed the value from 5.0 (default) to 50.0 $M_{\odot}$.
   (b) *metallicity-max* : Changed the value from 0.03 (default) to 0.000101 (closer to the default value of *metallicity-min*, which is 0.0001).

| Events and parameters | Stats |
|---|---|
| Merging DCOs | 25223 |
| **Merging BBHs** | **24395** |
| Merging BH-NSs | 828 |
| Merging BNSs | 0 |
| Mean of chirp masses of merging BBHs | 12.719 $M_{\odot}$ |
| Standard Deviation of chirp masses of merging BBHs | 3.741 $M_{\odot}$ |
| Mode of masses of merging BBHs | $\in [10,15]M_{\odot}$ |

Table 4.8: Summary of Run-4 Details

2. Comparing Run-3 and 4, the total number of merging BBHs has slightly decreased in Run-4.
3. Further, the average chirp mass of merging BBHs has slightly increased in Run-4 (an increase of $\sim 0.02M_{\odot}$). So, **decreasing the metallicity** (near to the default minimum) has indeed increased the chirp mass mean. However, the

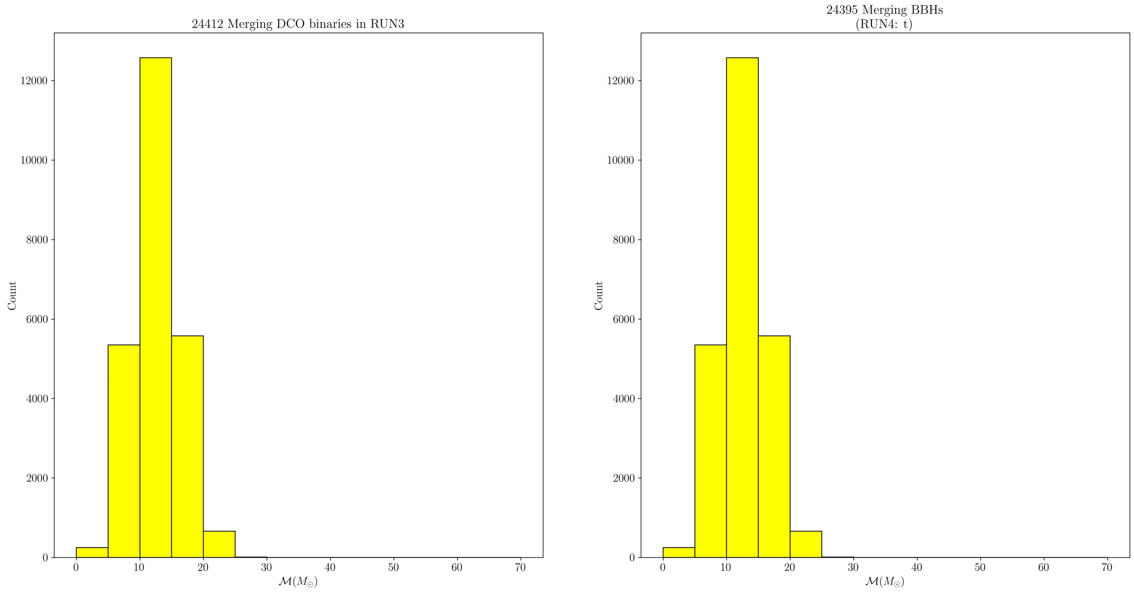


Figure 4.23: Run-3 vs Run-4:
It may seem like both the plots are exactly the same, but looking at them closely, they are not. The number of merging BBHs in $[0,5]M_\odot$ and $[5,10]M_\odot$ is more in Run-3 than Run-4, while the opposite is true in $[15,20]M_\odot$ and $[20,25]M_\odot$

standard deviation has decreased.

From this run, I got that decreasing the metallicity increases the chirp-masses. So, in the next few plots, I will try tweaking the mass and metallicity parameters further to get closer to the LIGO distribution.

**Run-5 (Constrains on mass and metallicity parameters)**

1. Parameters changed:
   (a) *initial-mass-min* : Changed the value from 5.0 (default) to 75.0 $M_\odot$.
   (b) *metallicity-max* : Set to 0.000112 (default = 0.0001)
   (c) *minimum-secondary-mass* : Changed the value from 0.1 (default) to 30.0 $M_\odot$

| Events and parameters | Stats |
|---|---|
| Merging DCOs | 16498 |
| **Merging BBHs** | **16496** |
| Merging BH-NSs | 2 |
| Merging BNSs | 0 |
| Mean of chirp masses of merging BBHs | 16.770 $M_\odot$ |
| Standard Deviation of chirp masses of merging BBHs | 2.949 $M_\odot$ |
| Mode of masses of merging BBHs | $\in [15,20]M_\odot$ |

Table 4.9: Summary of Run-5 Details

2. Finally, there is a significant increase in mean value. The peak has shifted to $[15,20]M_\odot$.

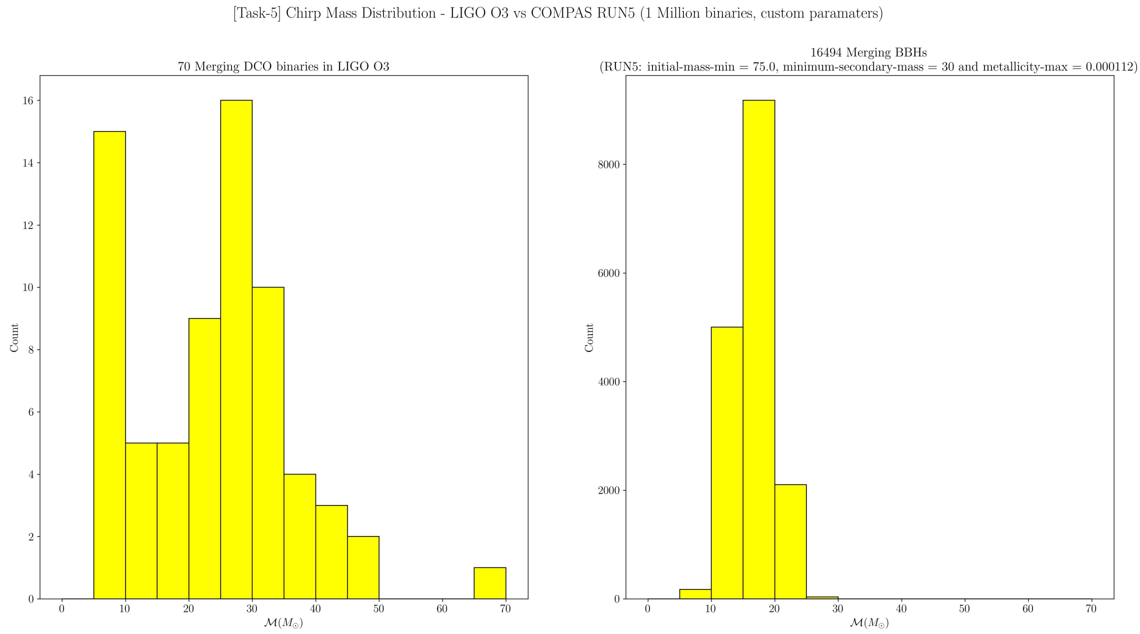


Figure 4.24: Run-5

**Run-6 (Constrains on mass and metallicity parameters)**

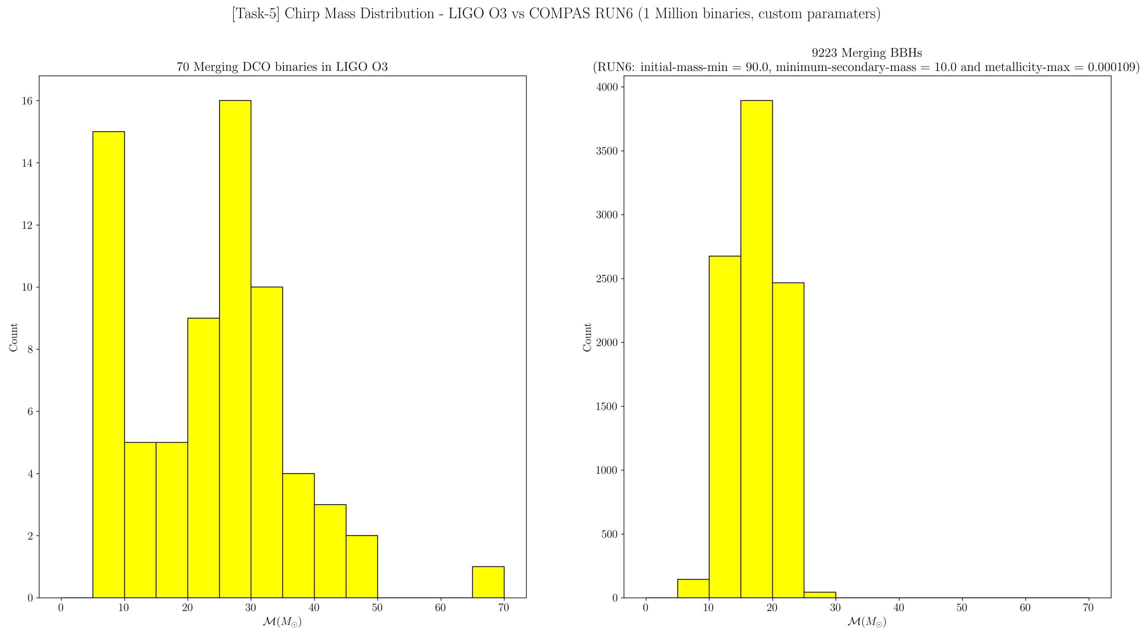


Figure 4.25: RUn-6

1. Parameters changed:
   (a) *initial-mass-min* : Changed the value from 5.0 (default) to 90.0 $M_{\odot}$.
   (b) *metallicity-max* : Set to 0.000109 (default = 0.0001)
   (c) *minimum-secondary-mass* : Changed the value from 0.1 (default) to 10.0 $M_{\odot}$

| Events and parameters | Stats |
|---|---|
| Merging DCOs | 9656 |
| **Merging BBHs** | **9223** |
| Merging BH-NSs | 433 |
| Merging BNSs | 0 |
| Mean of chirp masses of merging BBHs | 17.299 $M_\odot$ |
| Standard Deviation of chirp masses of merging BBHs | 3.359 $M_\odot$ |
| Mode of masses of merging BBHs | $\in [15,20]M_\odot$ |

Table 4.10: Summary of Run-6 Details

2. Compared to the previous, the total number of merging DCOs and merging BBHs have almost halved, while the number of merging BH-NSs has increased from 2 to 433 (this is due to the mass constraints I set in the previous task - primary masses had a minimum of 75 $M_\odot$ and secondary masses had a minimum of 30 $M_\odot$. Of course with this limit, there were only 2 formations of merging BH-NSs. Now however, with the limit on minimum of secondary masses reduced to 5 $M_\odot$, a lot more binaries would have become BH-NSs). The reason for the merging DCOs and BBHs to have decreased so much could be due to such a high mass limit for primary masses - 90 $M_\odot$ - most DCOs that formed couldn't have merged in Hubble time.
3. Compared to the previous run,
   (a) the percent of merging BBHs in the intervals $[10,15]M_\odot$ (32.9 % in Run-5 and 29.0 % here) and in $[15,20]M_\odot$ (51.0 % in Run-5 and 42.2% here) has decreased a bit.
   (b) While the percent has increased in the intervals $[20,25]M_\odot$ (11.4 % in Run-5 and 26.7% here) and $[25,30]M_\odot$ (0.163 % in Run-5 and 0.47 % here).
4. There is also a significant increase in the mean of the chirp masses of merging BBHs (16.770 to 17.299 $M_\odot$). This can be attributed to increasing the minimum initial primary masses from 75.0 to 90.0 $M_\odot$.

**Conclusion**

Overall, I varied the following parameters:
1. initial-mass-min
2. metallicity-max
3. secondary-mass-min

Further increasing the initial-mass-min would only result in a colossal decrease in the total number of merging BBHs (most DCOs that have formed with most of them being BBHs, wouldn't have merged in Hubble time). And, varying the metallicity by bringing it to near default minimum did increase the the average chirp mass, but it didn't have much of an effect in increasing the spread of the distribution.

So, this is how much close I could get to the chirp mass distribution from LIGO O3 data of 70 merging BBHs by varying various parameters in the simulation of a 1,000,000 binaries using COMPAS.

# 5. Bibliography

## 5.1 References


1. https://www.aavso.org/stellar-evolution
2. https://arxiv.org/pdf/1806.05820 (Mandel and Farmer's paper)
3. Evolution of Binary Systems by P Podsiadlowski
4. Population of Merging Compact Binaries Inferred Using Gravitational Waves through GWTC-3)
5. COMPAS Docs